

Tuning the Regio- and Stereoselectivity of C–H Activation in *n*-Octanes by Cytochrome P450 BM-3 with Fluorine Substituents: Evidence for Interactions Between a C–F Bond and Aromatic π Systems

Li-Lan Wu,^[a, b] Chung-Ling Yang,^[a, c] Feng-Chun Lo,^[a] Chih-Hsiang Chiang,^[a, b]
Chun-Wei Chang,^[a, b] Kok Yaoh Ng,^[a] Ho-Hsuan Chou,^[a] Huei-Ying Hung,^[a, b]
Sunney I. Chan,^[a] and Steve S.-F. Yu^{*[a, b]}

Abstract: We employed the water-soluble cytochrome P450 BM-3 to study the activity and regiospecificity of oxidation of fluorinated *n*-octanes. Three mutations, A74G, F87V, and L188Q, were introduced into P450 BM-3 to allow the system to undergo *n*-octane oxidation. In addition, the alanine at residue 328 was replaced with a phenylalanine to introduce an aromatic residue into the hydrophobic pocket to examine whether or not van der Waals interactions between a C–F substituent in the substrate and the polarizable π system of the phenylalanine may be used to steer the positioning of the substrate within the active-site pocket of the enzyme and control the regioselectivity and stereoselectivity of hydroxylation. Interestingly, not only

was the regioselectivity controlled when the fluorine substituent was judiciously positioned in the substrate, but the electron input into the iron–heme group became tightly coupled to the formation of product, essentially without abortive side reactions. Remarkable enhancement of the coupling efficiency between electron input and product formation was observed for a range of fluorinated octanes in the enzyme even without the A328F mutation, presumably because of interactions of the C–F substituent with the π system of the porphyrin macrocycle

within the active-site pocket. Evidently, tightening the protein domain containing the heme pocket tunes the distribution of accessible enzyme conformations and the associated protein dynamics that activate the iron porphyrin for substrate hydroxylation to allow the reactions mediated by the high-valent Fe^{IV}=O to become kinetically more commensurate with electron transfer from the flavin adenine dinucleotide (FAD)/flavin mononucleotide (FMN) reductase. These observations lend compelling evidence to support significant van der Waals interactions between the CF₂ group and aromatic π systems within the heme pocket when the fluorinated octane substrate is bound.

Keywords: C–H activation • cytochrome P450 • enzyme catalysis • fluorine • mutagenesis

Introduction

Cytochrome P450 BM-3 (CYP102A1) is a water-soluble monooxygenase with a flavin adenine dinucleotide (FAD)/

flavin mononucleotide (FMN) reductase^[1] that accepts reducing equivalents from nicotinamide adenine dinucleotide phosphate (NADPH) to activate O₂ at the heme iron and mediates the hydroxylation of saturated and unsaturated fatty acids with a chain length of 12 to 20 carbon atoms at their subterminal ends.^[2] Because of its high yield of heterologous overexpression in *Escherichia coli* and profound turnover efficiency,^[3] the BM-3 enzyme has been subjected to directed evolution for the activation of small alkanes,^[4] fine chemical conversions,^[5] and pharmaceutical lead optimization.^[6]

It is usually difficult to achieve activation of aliphatics by conventional synthetic methods due to the high C–H bond strength.^[7] However, it has been demonstrated that P450 BM-3 with the mutations A74G, F87V, and L188Q (3mt protein) hydroxylates *n*-octane into the 2-, 3-, and 4-ol with reasonable activity.^[8] Whereas the asymmetric environment within the active-site pocket offers opportunities to exploit amino acid substitutions to tune substrate specificity, it is seldom possible to accomplish controlled regioselectivity and stereoselectivity for a given substrate.^[5,9] Other strat-

[a] L.-L. Wu, C.-L. Yang, Dr. F.-C. Lo, C.-H. Chiang, C.-W. Chang, K. Y. Ng, Dr. H.-H. Chou, H.-Y. Hung, Prof. Dr. S. I. Chan, Dr. S. S.-F. Yu
Institute of Chemistry, Academia Sinica
Taipei 115 (Taiwan)
Fax: (+886) 2-2783-1237
E-mail: sfyu@chem.sinica.edu.tw

[b] L.-L. Wu, C.-H. Chiang, C.-W. Chang, H.-Y. Hung, Dr. S. S.-F. Yu
Department of Chemistry
National Cheng Kung University
Tainan 701 (Taiwan)

[c] C.-L. Yang
Graduate Institute of Engineering
National Taiwan University of Science and Technology
Taipei 106 (Taiwan)

Supporting information for this article is available on the WWW under <http://dx.doi.org/10.1002/chem.201003631>.

gies need to be developed to achieve highly regioselective and stereoselective chemical conversions.

Research in our laboratory has been directed toward understanding the effects of fluorinated substituents on the regio- and stereoselectivity of oxidation of aliphatics mediated by pMMO from *Methylococcus capsulatus* (Bath)^[10] and cytochrome P450 BM-3 from *Bacillus megaterium*. Fluorine substitution can usually improve the penetration of aliphatics through the membranes, tune pK_a values to render them more biologically compatible, and enhance their metabolic stability.^[6b,11] Metabolic stability is especially susceptible in cytochrome P450 proteins.^[11a,12] However, much less is known about the effects of a fluorinated substituent on the stereochemical control of substrate oxidation by P450. In terms of electronegativity and dipole moment, the C–F bond is similar to the C–OH bond. Molecules containing a C–F bond typically prefer positively polarized environments to form C–F...H–N, C–F...C=O, and C–F...H–C $_{\alpha}$ associations.^[11b] However, there are many examples in biological systems that suggest that the C–F bond is more similar to the C–H bond.^[10,13] Because of the bioisosteric property, fluorinated compounds have also become pharmaceutically significant for lead optimization.^[6b,11] Organofluorine derivatives of potential inhibitors or drugs are also extensively used as therapeutics targeted at proteins and cellular enzymes.^[11,13b]

In this study, we have introduced one, two, or three fluorine atoms into specific carbon positions of the *n*-octane molecule to study the effects of the fluorinated substrate on the oxidation. To achieve fluorination at specific carbon positions, we have considered the two powerful nucleophilic fluorinating reagents bis(2-methoxyethyl)aminosulfur trifluoride (Deoxo-Fluor) and diethylaminosulfur trifluoride (DAST).^[14] Deoxo-Fluor appears to be a somewhat more effective fluorinating reagent than DAST because of its significantly higher thermal stability and greater reactivity. Generally, Deoxo-Fluor readily converts alcohols into alkyl fluorides, aldehydes/ketones into *gem*-difluorides, and carboxylic acids into the corresponding trifluoromethyl derivatives.

If P450 activity toward the oxidation of aliphatics is maintained, or even becomes enhanced, with fluorinated substituents, then most likely, these bioisosteric derivatives would behave just like the parent *n*-octanes when encapsulated into the hydrophobic pocket of the enzyme. Any stabilization of the fluorinated substrate or enhancement in the oxidation of octane would presumably come from additional electrostatic interactions, such as hydrogen-bonding and dipole–dipole interactions, and/or van der Waals interactions (dipole–induced-dipole and London dispersive forces) of the polar C–F bonds with residues lining the heme pocket. Unlike hydrogen-bonding or dipole–dipole interactions, van der Waals interactions do not usually provide specific directionality or orientations like hydrogen bonding. Moreover, the strengths are smaller than hydrogen bonding, typically in the range of about 0.02–2.0 kcal mol⁻¹,^[15] but these interactions are highly dependent on the shape and volume of the interacting molecular partners. To illustrate, we cite two

examples. Recently, we have demonstrated that 1,1,1-trifluoropropane and -propene can also serve as substrates for the particulate methane monooxygenase from *Methylococcus capsulatus* (Bath), with varied chiral selectivity or greater stereoselectivity than the corresponding parent hydrocarbons.^[10] The regioselectivity of the hydroxylation of 5,5-difluorocamphor by cytochrome P450cam is dramatically changed from 5-*exo* to C-9.^[16] Herein, we show that it is also possible to tune the reactivity, regioselectivity, and stereoselectivity of the hydroxylation of octane by the P450 BM-3 3mt enzyme by the introduction of fluorinated substituents.

Results

Preparation of fluorinated *n*-octanes: A series of designed and synthesized fluorinated *n*-octanes **1–7** (Schemes 1 and 2) were deployed as the substrates for the P450 BM-3 variants. 1-Fluorooctane (**5**) was obtained from Sigma–Aldrich. Fluorinated octanes **1–4** and **6** were prepared by employing the fluorination reagent Deoxo-Fluor (Matrix Scientific) in CH₂Cl₂ (Supporting Information).^[14a] 1-Octanal (**8**); 1,8-octandiol (**12**); and 2-, 3-, and 4-octanone (**9–11**) were used as the starting materials to generate the corresponding products, 1,1-, 2,2-, 3,3-, and 4,4-difluorooctanes (**1–4**) and 1,8-difluorooctane **6**, respectively. (Table S1 in the Supporting Information)

Product formation was monitored by gas chromatography (GC) and gas chromatography/mass selective detector (GC/MSD) at 100 °C under isothermal conditions (see the Supporting Information). We observed **1–4** and **6** at t_R = 4.24, 3.97, 4.06, 4.00, and 5.99 min, respectively, whereas **8–12** appeared at t_R = 6.56, 6.46, 6.33, 6.02, and 15.32 min, respectively, under the same separation conditions. Mass spectral analysis of **1–4** did not reveal a signal with molecular mass m/z 150. Among the molecular mass fragments, we usually observed a signal at m/z 130 corresponding to the elimination of hydrogen fluoride during ionization. Mass fragments were also detected at m/z 135 and 121, which were derived from the mass fragmentation of **2** and **3**, respectively. These two signals represented the mass fragment CH₃(CH₂)₅CF₂⁺ and CH₃(CH₂)₄CF₂⁺, respectively, which confirmed the formation of the target products, 2,2-difluorooctane and 3,3-difluorooctane.

The fluorinated products were further identified by ¹H, ¹³C, and ¹⁹F NMR spectroscopy (see the Supporting Information). A ¹H NMR signal with a chemical shift at δ = 5.77 ppm (tt, 57.2 and 4.4 Hz) for the primary carbon indicated the formation of **1**. Similarly, triplets in the ratio of 1:2:1 with splitting constants of 8.0 and 18.4 Hz, 6.8 and 7.6 Hz, and 8.0 and 8.0 Hz also appeared at δ = 0.86 and 1.55 ppm, δ = 0.87 and 0.98 ppm, and δ = 0.90 and 0.94 ppm, respectively, for the methyl groups of **2–4**, respectively, after fluorination. Evidently, we had incorporated two F atoms specifically at the target carbon position. Furthermore, compound **6**, with two hydrogen atoms at the primary carbon, gave a ¹H NMR signal at δ = 4.41 ppm (dt, 47.4 and 6.0 Hz).

ated sufficient quantities of products to facilitate separation and structural characterization. In all cases, the products consisted of a mixture of secondary alcohols (Schemes 1 and 2, and Schemes S3 and S4 in the Supporting Information). The position of hydroxylation of the fluorinated octane was established in each case by EI-MS through identification of the molecular fragments derived from cleavage of the C–C bonds adjacent to the oxygen of the alcohol. The structures of the products were further characterized by ^1H , ^{13}C , and ^{19}F NMR spectroscopy; GC; and GC/MSD.

When **1** was used as the substrate, we observed mass fragments from the products **1a–d** at m/z 151, 137, 123, and 109, corresponding to $\text{CHF}_2(\text{CH}_2)_n\text{OH}^+$ ($n=3–6$), respectively, indicating hydroxylation of **1** at the positions $\omega-1$ to $\omega-4$. Applying the same strategy enabled us to identify the sites of oxidation of **2**, **3**, and **4** to give the products **2a–2c**, **3a**, **3b**, and **4a** (Scheme 1).

When monofluorinated octane **5** (purchased from Sigma–Aldrich) was used as the substrate for 3mt catalysis, EI-MS analysis of the product alcohols revealed signals at m/z 133, 119, 105, and 91, which indicated hydroxylation at $\omega-1$ to $\omega-4$, respectively, through C–H activation of **5a–5d** (Scheme 2). For **6**, the major products were **6b** and **6c**, as evidenced by signals at m/z 119 and 105, respectively, in a ratio of about 1:1 corresponding to $\omega-2$ and $\omega-3$ activation. There was only very minor $\omega-1$ activation observed in this case.

In the ^1H NMR spectra, the fluorine atoms associated with the fluorinated substituent in the fluorinated octanols should be strongly spin-coupled to their neighboring protons two and three bonds away and give rise to large $^{19}\text{F}/\text{H}$ spin-spin splitting. The enzymatically converted fluorinated products **1a–1d** had a terminal CHF_2 group adjacent to a CH_2 group in each case. These ^1H NMR signals appeared at $\delta=5.77–5.84$ ppm (**1a**: $\delta=5.77$ ppm; **1b**: $\delta=5.77$ ppm; **1c**: $\delta=5.78$ ppm; **1d**: $\delta=5.84$ ppm) as a superposition of two sets of triplets with coupling constants of 56.8–57.2 and 4.0–4.4 Hz, (**1a**: $J=57.2$ and 4.0 Hz; **1b**: $J=57.2$ and 4.0 Hz; **1c**: $J=56.8$ and 4.4 Hz; **1d**: $J=56.8$ and 4.4 Hz), respectively. The CH_3 groups in products **2a–2c** were coupled to two vicinal ^{19}F nuclei in each case, and the ^1H NMR absorption appears as a triplet at $\delta=1.55–1.58$ ppm (**2a**: $\delta=1.55$ ppm; **2b**: $\delta=1.58$ ppm; **2c**: $\delta=1.55$ ppm) (Scheme 1 and Scheme S3 in the Supporting Information). For product **5a**, the ^1H NMR spectrum showed a doublet of triplets at $\delta=4.42$ ppm. The two coupling constants, $J=45.0$ and 6.0 Hz, corresponded to the coupling of the proton of the CH_2F group to the terminal fluorine atoms and to an adjacent CH_2 group. Similar signals were observed in the ^1H NMR spectra of these products, at $\delta=4.39$ (dt, 2H, $J=47.1$ and 6.0 Hz) and 4.71–4.05 ppm (m, 2H) for **6b**, and at $\delta=4.42$ (dt, 2H, $J=47.2$ and 6.0 Hz) and 4.45 ppm (dt, 2H, $J=47.1$ and 5.6 Hz) for **6c**. These spectral features arose from β - and γ -hydroxylation relative to the terminal fluorine substituents in **6b** and **6c**. In products **3a**, **3b**, and **4a**, one of the CH_3 groups exhibited coupling adjacent to a CH_2 group that is proximal to the two fluorine atoms substituted at the

C-6 and C-5 carbon atoms, respectively. The ^1H absorption of these protons appeared as triplets at $\delta=0.98$, 0.98, and 0.94 ppm, with weak coupling constants of $J=7.5$, 7.5, and 7.2 Hz, for **3a**, **3b** and **4a**, respectively.

Other features in the ^1H NMR spectra showed no interference from the fluorine atoms. Upon the formation of octan-2-ol derivatives **1–5a**, the protons of one of the terminal CH_3 groups in each secondary alcohol were coupled with the $\text{CH}(\text{OH})$ group proton to give a doublet in the ^1H NMR spectra at $\delta=1.16–1.28$ ppm (**1a**: $\delta=1.16$ ppm; **2a**: $\delta=1.17$ ppm; **3a**: $\delta=1.17$ ppm; **4a**: $\delta=1.21$ ppm; **5a**: $\delta=1.28$ ppm) with coupling constants ranging from $J=4.0$ to 6.3 Hz (**1a**: $J=6.0$ Hz; **2a**: $J=4.0$ Hz; **3a**: $J=6.3$ Hz; **4a**: $J=6.0$ Hz; **5a**: $J=6.0$ Hz). For each of the product alcohols **1a–d**, **2a–c**, **3a**, **3b**, **4a**, **5a**, **6b**, and **6c**, there was one new downfield absorption feature in the ^{13}C NMR spectra appearing in the range from $\delta=67.50$ to 72.95 ppm (**1a**: $\delta=68.0$ ppm; **1b**: $\delta=72.9$ ppm; **1c**: $\delta=71.2$ ppm; **1d**: $\delta=71.1$ ppm; **2a**: $\delta=67.9$ ppm; **2b**: $\delta=73.0$ ppm; **2c**: $\delta=71.0$ ppm; **3a**: $\delta=67.8$ ppm; **3b**: $\delta=72.7$ ppm; **4a**: $\delta=67.5$ ppm; **5a**: $\delta=68.1$ ppm; **6b**: $\delta=68.3$ ppm; **6c**: $\delta=71.2$ ppm), which was readily assigned to the carbon of the $\text{CH}(\text{OH})$ group, providing strong evidence for the formation of secondary alcohol by the enzymatic conversion.

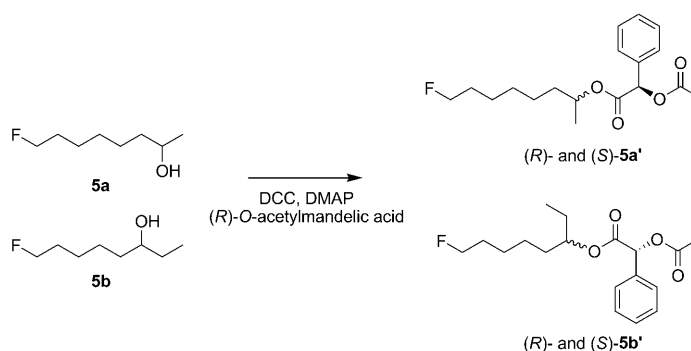
The products **1a–d**, **2a–c**, **3a**, **3b**, **4a**, **5a**, **6b**, and **6c** all gave eight distinct signals in the ^1H spin-decoupled ^{13}C NMR spectra, indicating that they were straight-chain octanol derivatives. The downfield 1:2:1 triplet appearing at $\delta=117.3–4$, (**1a**: $\delta=117.4$ ppm; **1b**: $\delta=117.3$ ppm; **1c**: $\delta=117.3$ ppm; **1d**: $\delta=117.4$ ppm), 124.3–4 (**2a**: $\delta=124.3$ ppm; **2b**: $\delta=124.3$ ppm; **2c**: $\delta=124.4$ ppm), 125.4–6 (**3a**: $\delta=125.4$ ppm; **3b**, $\delta=125.6$ ppm), and 125.2 ppm (**4a**), with extremely large splitting constants of $J=235.0–239.0$ Hz (**1a**: $J=238.0$ Hz; **1b**: $J=237.0$ Hz; **1c**: $J=237.0$ Hz; **1d**: $J=237.0$ Hz; **2a**: $J=236.0$ Hz; **2b**: $J=237.0$ Hz; **2c**: $J=235.0$ Hz; **3a**: $J=239.0$ Hz; **3b**: $J=239.0$ Hz; **4a**: $J=238.0$ Hz) (Scheme 1 and Scheme S3 in the Supporting Information) for compounds **1a–d**, **2a–c**, **3a**, **3b**, and **4a**, indicating that there were two fluorine atoms substituted at the C-1, C-2, C-3, and C-4 positions of the secondary octanol derivatives, respectively. On the other hand, **5a**, **6b**, and **6c** all displayed a strong 1:1 splitting pattern with coupling constants of $J=163.0–4.0$ Hz (**5a**: $J=164.0$ Hz; **6b** and **6c**: both with $J=163.0$ Hz) (Scheme 2 and Scheme S4 in the Supporting Information). There was only one such pattern for **5a** appearing at $\delta=84.13$ ppm. However, both **6b** and **6c** showed two similar pairs of doublets at $\delta=83.96$ and 81.66 ppm and $\delta=84.14$ and 83.94 ppm, respectively. These observations were consistent with one terminal CH_2F in **5a** and two in **6b** and **6c**, which corresponded to the CH_2F groups at the C-1 and C-8 positions of the octanol derivatives, respectively.

We noted that the two fluorine atoms of CF_2 in **1d**, **2c**, **3b**, and **4a** became diastereotopic when the chiral hydroxylation occurred at a carbon within three C–C bonds. Therefore, for products **1d**, **2c**, **3b**, and **4a**, we observed two signals in the ^{19}F NMR spectra with equal intensities at $\delta=$

–115.88 and –116.14 ppm, $\delta = -90.92$ and -91.28 ppm, $\delta = -100.50$ and -100.61 ppm, and $\delta = -98.17$ and -98.25 ppm, respectively, due to the appearance of two inequivalent ^{19}F nuclei.

Finally, it was difficult to separate products **5b–5d** by gravity column chromatography. Only minor amounts of **6a** were formed. The product yields of **7** were also lower than those obtained for the other substrates. Therefore, we could only identify these products through GC and GC/MSD at the present time.

P450 BM-3 3mt A328F mutant mediated regioselective hydroxylation of the fluorinated *n*-octanes at the C-2 position: In the case of the 3mt A328F mutant, we found that the major product of *n*-octane activation was 2-octanol as predicted (94% abundance, Table 1).^[9b,20] Unsurprisingly, the



Scheme 3. Fluorinated alcohols **5a** and **5b** were further derivatized by *(R)*-O-acetylmandelic acid.

Table 1. The throughputs of secondary alcohol formation were obtained from ratios of the hydroxylated products produced by purified P450 BM-3 3mt (GVQ) and 3mt F328 (GVQF) by using *n*-octane and **1–7** as the substrates.

Substrates	P450 BM-3 3mt (GVQ)				P450 BM-3 3mt F328 (GVQF)		
	2-ol [%] (<i>ee</i> [%]) ^[a]	3-ol [%] (<i>ee</i> [%]) ^[a]	4-ol [%]	5-ol [%]	2-ol [%] (<i>ee</i> [%]) ^[a]	3-ol [%]	4-ol [%]
<i>n</i> -octane	28 (20)	43 (39)	29	n.d. ^[c]	94 (43)	6.0	n.d. ^[c]
1	32 (60, 56 ^[b])	42 (65)	16	10	97 (38, 33 ^[b])	2.9	n.d. ^[c]
2	22 (56, 56 ^[b])	48 (70, 80 ^[b])	30	n.d. ^[c]	97 (70, 67 ^[b])	2.6	n.d. ^[c]
3	22 (64, 67 ^[b])	78 (79, 80 ^[b])	n.d. ^[c]	n.d. ^[c]	96 (43, 43 ^[b])	4.0	n.d. ^[c]
4	100 (52, 56 ^[b])	n.d. ^[c]	n.d. ^[c]	n.d. ^[c]	100 (70, 67 ^[b])	n.d. ^[c]	n.d. ^[c]
5	23 (58, 60 ^[b])	43 (61)	20	14	97 (31, 33)	2.6	n.d. ^[c]
6	1.9	46	52	n.d. ^[c]	n.d.	n.d. ^[c]	n.d. ^[c]
7	51	32	17	n.d. ^[c]	88	4.1	7.8

[a] The *ee* ($ee = (RR - SR)/(RR + SR)$) ratios of the diastereomeric *(R)*-O-acetylmandelic acid derivatives were determined by the corresponding signal areas appearing in GC/MSD chromatograms. [b] The *ee* ratios were determined by the ratios of the integrated areas of the stereoselective shifted methyl resonances in the ^1H NMR spectra for the *(R)*-O-acetylmandelic acid derivatives derived from *(R)*- and *(S)*-**1–5a'**, **1–3**, and **5b'**. [c] n.d. = not detected.

major products for the fluorinated substrates **1–7** were also activated at subterminal carbon atoms, resulting in the formation of fluorinated octan-2-ol derivatives **1a–5a** and **7a**. However, there was no detectable product derived from **6**. Other than this, the reactions were actually well controlled to give the ω -1 alcohol distal to the fluorine substituent.

Stereoselectivity of the subterminal activation of the fluorinated *n*-octanes mediated by P450 BM-3 3mt and 3mt A328F: In principle, the surface roughness of the hydrophobic pocket could be modified upon the introduction of an aromatic residue at amino acid 328 and changing the *ee* ratios of the fluorinated ω -1 products formed by activation of the fluorinated octanes by the 3mt enzyme and the A328F mutant. To compare the stereoselectivity of hydroxylation of 3mt and 3mt-F328, we esterified the converted **1a–5a** into the diastereomeric *(R)*-O-acetylmandelic acid derivatives (Schemes 1 and 3). The absolute configurations at C-2 for each of the octan-2-ol derivatives (*R*)- and (*S*)-**1–5a'** were then determined from the chemical shift of the C-1 methyl terminus. The anisotropic magnetic susceptibility of the

proximal phenyl substituent acted as a chiral resolving reagent and exerted an upfield shift of the corresponding terminal methyl group protons in the ^1H NMR spectra for the product in the *S* configuration.^[10,21] In this manner, we could determine the *ee* ratios. Commercially available (*S*)- and (*R*)-octan-2-ol (Sigma–Aldrich) were employed as authentic standards of the *(R)*-O-acetylmandelic acid derivatives (see the Supporting Information). As shown in the ^1H NMR spectrum, the absorption of the terminal methyl for the (*S*,*R*)-octan-2-ol ester occurred at $\delta = 1.05$ ppm, which was $\delta =$

0.16 ppm upfield of the parent (*R,R*)-octan-2-ol ester ($\delta = 1.21$ ppm). Similar patterns were observed from the product alcohols derived from substrates **1–5** mediated by both P450 BM-3 variants (Table S1 in the Supporting Information). In the ω -1 products, the methyl group of the fluorinated (*S,R*)-octan-2-ol esters derived from (*S*)-**1–5a'** were also shifted upfield $\delta = 0.12$ – 0.18 ppm relative to that of the (*R,R*)-derivatives derived from (*R*)-**1–5a'**. The stereochemical results were verified by GC by comparison with the retention times of the product octanols with authentic standards.

The five fluorinated octanes **1–5** all showed higher stereoselectivity toward the *R* configuration with comparable ratios for their ω -1 products (56–67% *ee* by NMR spectroscopy and 52–64% *ee* by GC) when the conversion was carried out by the 3mt protein (Table 1). However, in the case of the 3mt F328 protein, the *ee* ratios of the ω -1 products obtained for substrates **2** and **4** increased significantly to 67–70% *ee* according to both GC and NMR spectroscopy. In contrast, the corresponding *ee* ratios decreased to 31–43% *ee* for the C-1 fluorinated **1** and **5** as well as the C-3 fluorinated **3**. For comparison, the *ee* ratios of the product

(*R*)-octan-2-ols and (*S*)-octan-2-ols derived from *n*-octane mediated by 3-mt and 3-mt A328F proteins were 20 and 43% *ee*, respectively, according to GC by comparison with the retention times of authentic standards. It was not possible to ascertain the stereoselective ratios by NMR spectroscopy here due to the relatively poor yields of the corresponding conversions when using *n*-octane. From these results, it is evident that the influence of Phe328 on the stereochemical outcome of the ω -1 hydroxylation of the various fluorinated octanes mediated by the A328F 3mt protein is manifested only every other CF₂ substituent along the hydrocarbon chain in an alternating fashion, beginning with C-2.

We have also compared the stereoselectivity of the hydroxylation of C-3 in octane and the ω -2 hydroxylation of the fluorinated octanes mediated by the BM-3 3mt enzyme. (Table 1 and Table S1 in the Supporting Information). To accomplish this, we examined the diastereomeric (*R*)-*O*-acetylmandelic acid derivatives of (*R*)- and (*S*)-octan-3-ols and their corresponding fluorinated alcohols by NMR spectroscopy. Derivatization of (*S*)-octan-3-ol (Sigma–Aldrich) with (*R*)-*O*-acetylmandelic acid gave two ¹H NMR spectroscopy signals for the terminal methyl groups at δ = 0.56 and 0.85 ppm, respectively (Supporting Information). From the corresponding ¹H NMR spectroscopy signals obtained from the derivatives of (\pm)-octan-3-ol (the racemic mixtures of (*R*)- and (*S*)-octan-3-ols), the terminal methyl groups of the (*R*)-octan-3-ol derivative were observed at δ = 0.74 and 0.87 ppm. From the chemical shifts of the terminal methyl groups adjacent to *gem*-difluorination at C-7 of (*R*)- and (*S*)-octan-3-ol **2b'** appearing at δ = 1.38 ppm with a coupling constant of *J* = 21 Hz, we could identify the corresponding ¹H NMR absorption of the other methyl groups proximal to the hydroxylation positions for (*R*)- and (*S*)-**2b'** at δ = 0.88 and 0.57 ppm, respectively; a 0.31 ppm upfield shift for (*S*)-3-ol **2b'** relative to enantiomer (*R*)-**2b'** (Table S1 in the Supporting Information). Comparable stereoselective anisotropic shift patterns were observed for the parent authentic standards octan-3-ol (*R*-*S*: δ = 0.31 ppm, see the Supporting Information) and **3b'** (*R*-*S*: δ = 0.30 ppm).

The (*R,R*)- and (*S,R*)-octan-3-ol derivatives could also be separated by GC and the retention times were 89 and 90 min, respectively (see the Supporting Information). In the GC chromatograms, the order of appearance based on the retention times was (*R*)-**1b'**, **-2b'**, and **-3b'** (*t_R* = 192, 164, and 148 min, respectively) always ahead of (*S*)-**1b'**, **-2b'**, and **-3b'** (*t_R* = 195, 166, and 149 min, respectively; Table S1 in the Supporting Information). On the basis of these observations,

we concluded that the octan-3-ol product *ee* ratio was 39% in favor of the *R* configuration in the case of *n*-octane (Table 1). Substrates of the fluorinated octanes **1–3** and **5** gave even better enantiomeric selectivity toward the *R* configuration with *ee* ratios in the range 61–80%.

Dramatic high coupling efficiencies between electron transfer and substrate activation in the P450 BM-3 variants for the fluorinated substrates: To analyze the specific activities of the two P450 variants quantitatively, we purified the two proteins to homogeneity by using a HisTrap HP column (GE Healthcare). The fluorinated octanes **1–7** were subjected to the purified enzyme preparations for 1.0 min conversions at room temperature. For each substrate, the throughputs of the various product secondary alcohols are summarized in Table 1 for 3mt and the A328F variant. The corresponding specific activities of the purified proteins are expressed in terms of the rate of NADPH consumption and the rate of product formation (molecules of NADPH or molecules of product alcohol formed per enzyme per min) and are given in Table 2. In case of the 3mt, the rates of

Table 2. Rates of NADPH consumption, product formation, and the corresponding coupling efficiencies were measured for P450 BM-3 3mt (GVQ) and 3mt F328 (GVQF) by using *n*-octane and **1–7** as the substrates.

Substrates	NADPH consumption [min ⁻¹] ^[a,b]		Product formation [min ⁻¹] ^[b]		CE ratio ^[c] [%]	
	3mt	3mt F328	3mt	3mt F328	3mt	3mt F328
<i>n</i> -octane	1608 ± 80	1034 ± 52	150 ± 14	215 ± 14	9.3	21
1	1809 ± 171	744 ± 51	1765 ± 89	610 ± 34	98	82
2	1809 ± 57	653 ± 24	1617 ± 150	491 ± 32	89	75
3	1326 ± 57	619 ± 28	993 ± 64	446 ± 19	75	70
4	1795 ± 46	1759 ± 107	1289 ± 68	1197 ± 104	72	68
5	2010 ± 113	2012 ± 128	1758 ± 149	1647 ± 150	88	82
6	2010 ± 80	1085 ± 106	769 ± 14	n.d.	38	n.d.
7	1085 ± 57	857 ± 43	442 ± 27	433 ± 13	41	51

[a] Protein concentrations were quantified by CO-binding difference spectra of the reduced heme by using an extinction coefficient of 91 mm⁻¹cm⁻¹ for the 450 minus 490 nm signals.^[9b] [b] The background NADPH consumption rate (without substrate) was (266 ± 2.4) min⁻¹. [c] CE = coupling efficiency.

NADPH consumption (160 nM protein, 320 μM NADPH, 13 mg bovine liver catalase, and 4.0 mM substrates)^[9b] ranged from 1085–2010 min⁻¹ for substrates **1–7**, similar to the consumption rate previously reported for *n*-octane (1760 min⁻¹)^[22] and repeated in the present study ((1608 ± 80) min⁻¹) as a control. In contrast, the rates of product formation from substrates **1–7** (160 nM protein, 320 μM NADPH, 13 mg bovine liver catalase, and 4.0 mM substrates),^[9b] which ranged from 442 to 1765 min⁻¹, were significantly higher than the corresponding rate for *n*-octane (150 min⁻¹). Thus, the incorporation of a fluorine substituent has greatly improved the coupling of electron transfer to compound conversion in the 3mt protein. The coupling efficiency (CE ratio) ranged from 38 to 98% in the case of the fluorinated octanes compared with a mere 9.3% for *n*-octane.

Further insights into the influence of the fluorine substituents on the C–H activation of *n*-octane were provided by the data obtained on the 3mt A328F mutant. Here, except

for substrates **4** and **5**, the NADPH consumption rates decreased by a factor of about 1/3 to 4/5 relative to the 3mt. However, there was a corresponding drop in the rate of product formation, so that the CE ratios were not dramatically affected (only a change of $\approx 10\%$ relative to the 3mt protein). In the case of substrates **4** and **5**, the NADPH consumption and product formation rates were, in fact, comparable so that the CE ratios were essentially the same for the two enzymes. Thus, although these substrates exhibited the same regioselectivity as *n*-octane in favor of formation of the 2-ol, the product throughputs and the corresponding coupling efficiencies were substantially different.

Discussion

The activation of the P450 enzyme for substrate oxidation requires the initial expulsion of water from within the hydrophobic pocket. This process, which is accompanied by the binding of a substrate molecule, switches the heme iron from six to five coordinate, and raises the redox potential of the iron to facilitate the transfer of an electron from NADPH to reduce the heme iron for subsequent dioxygen activation.^[7b,23] Clearly, the sequestering of the substrate into the heme pocket requires cooperation of the iron porphyrin with the residues lining the substrate channel (Figure 1).

There have been attempts to discern the location and spatial orientations of the substrates in the crystal structures of P450 BM-3 to delineate those features of the hydrophobic pocket that might control the regio- and stereoselectivity of the C–H activation. The bound substrates have always been encapsulated at a site within a pocket some 6–8 Å above (distal) the iron porphyrin. Accordingly, these structural results have not provided the desired insight into how interactions between the substrate and the iron porphyrin might contribute to the control of the oxidation.^[20,24]

Evidence for the existence of a distinct pocket for the binding of the substrate not associated with the polycyclic porphyrin system has mainly come from X-ray crystallographic studies. In the cytochrome P450 (BM-3, 3mt, and 3mt F328) proteins, this site is formed by the amino acids Ser72, Ala74 (Gly74 for 3mt), Leu75, Val78, Ala82, Phe87 (Val87 for 3mt), Thr88, Leu181, Ile259, Thr260, Ile263, Ala264, Thr268, Ala328 (Phe328 for 3mt F328), Ala330, Thr348, Met354, Leu437, and Thr438. The natural substrates of the wild-type enzyme are C₁₂ and C₁₄–C₁₆ fatty acids, and these fatty acids are typically hydroxylated at the ω -1, ω -2, and ω -3 positions with stereoselectivities of 86–99, 86–96, and 44–74% *ee*, respectively, toward the formation of the secondary alcohol in the *R* configuration.^[24–25] Two wild-type structures, 1JPZ^[23] and 1FAG,^[26] are shown in Figure 2. In these structures, the shortest distance of the C–H bond to the heme iron occurs at the ω -3 carbon (6–8 Å). For the purpose of this discussion, we can set the position of this carbon in *N*-palmitoylglycine or palmitoleic acid as the stereocenter for the recognition of the aliphatic chain

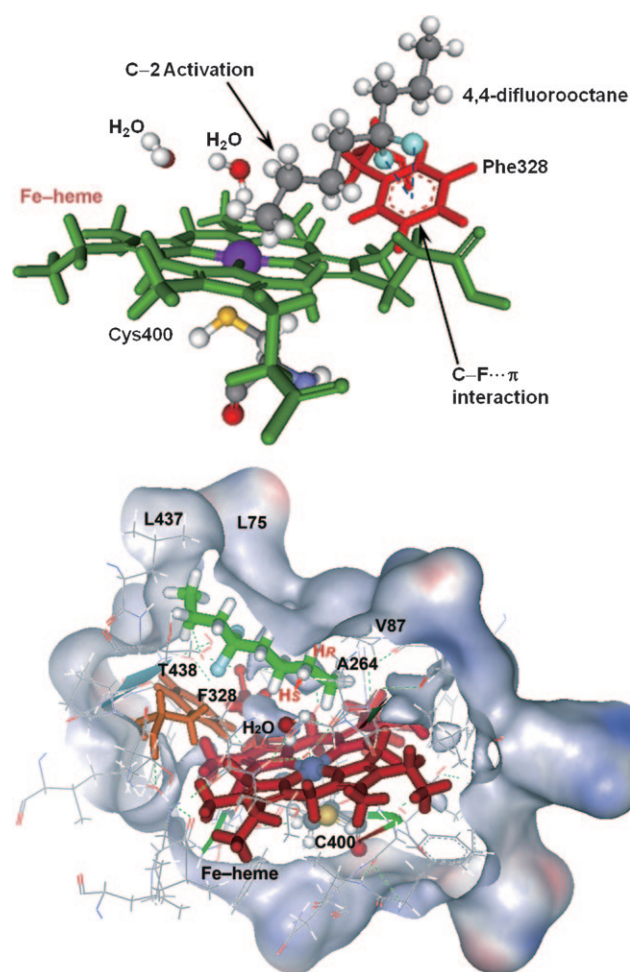


Figure 1. Three-dimensional models (PDB code 1JPZ, modified by Discovery Studio 2.0 (Accelrys)) show the encapsulation of substrate **4** within the pocket of P450 BM-3 with F328 to generate the proposed CF₂··· π interaction and the heme iron mediating the regioselective ω -1 oxidation.

(Figure 2). The remainder of the secondary substrate pocket can be divided into three zones: large (L), medium (M), and small (S). Most likely, the S zone is located at the small cleft around the positions F87 (wild type) or V87 (3mt). When octane is used as the substrate in BM-3 3mt, the principal product is the secondary alcohol at C-3 (Figure 3). Thus, for this small substrate, we expect the aliphatic chain to have a principal binding site in the M and L zones, with the ethyl group in the M zone and the pentyl group in the L zone. However, there should be a distribution of binding sites, corresponding to moving the aliphatic chain into other sites within these two zones. Given the location and size of the M zone from the crystal structures, the maximum hydrocarbon chain length for this cavity would be *n*-propyl or *n*-butyl. If the hydroxylation of the hydrocarbon occurs with the substrate more or less in place, then the regioselectivity will be determined by the distribution of binding sites in the M and L zones. This distribution is controlled by the energetics associated with the substrates occupying different binding

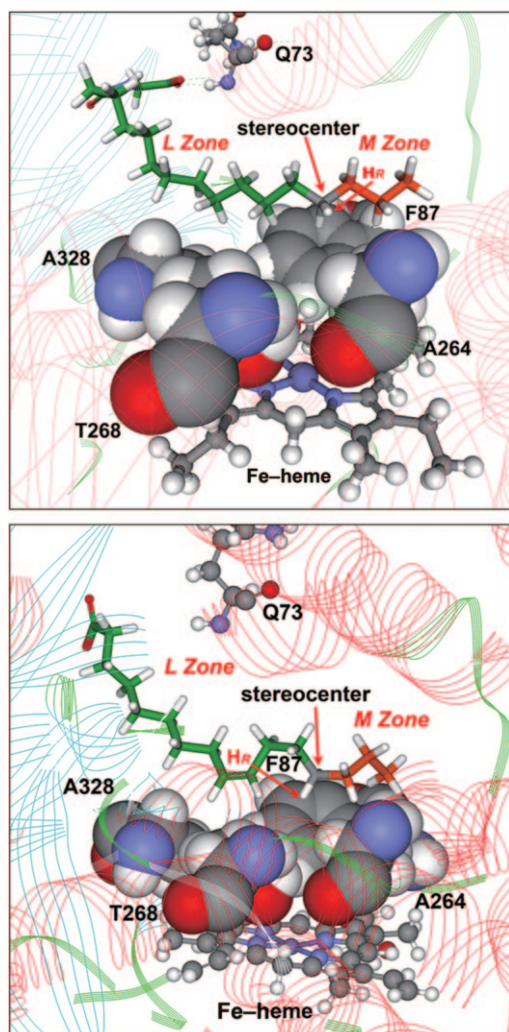


Figure 2. The hydrophobic pocket of P450 BM-3 for substrates *N*-palmitoylglycine or palmitoleic acid, respectively, reproduced from PDB codes 1JPZ (a) and 1FAG (b) by Discovery Studio 2.0 (Accelrys). L and M refers to the large and medium zones, respectively.

sites. This analysis provides a reasonable scenario for hydroxylation at C-2, C-3, and C-4 of octane in the case of the BM-3 3mt enzyme, and hydroxylation at ω -1, ω -2, ω -3, and ω -4 with **1** and **5** (Table 1 and Schemes 1 and 2). For the remaining fluorinated octanes, when the fluorine substituent is moved to internal carbon atoms, as in the case of substrates **2**, **3**, and **4**, the distribution of products is now restricted by the location of the fluorine substitution, and in the case of **4**, hydroxylation is totally regioselective to yield only the 2-ol (Figure 3). When the substrate is switched to **6**, oxidation at C-2 becomes negligible. It is interesting to note that the α and/or β positions to the fluorinated carbon atoms within the octane derivatives **1–7** are not susceptible to oxidation by 3mt protein (see throughput data in Table 1, Schemes 1 and 2, and Schemes S3 and S4 in the Supporting Information).

In the above model, as long as the C–H_R bonds are presented directly to the activated high-valent iron–oxo species,

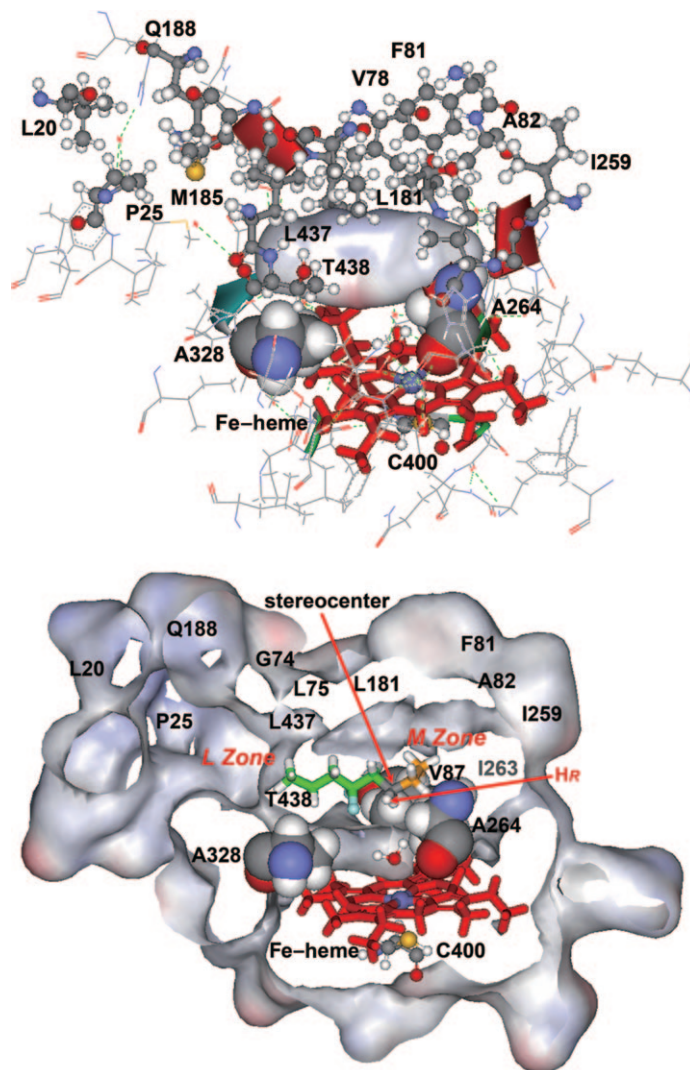


Figure 3. Three-dimensional models (PDB code 1JPZ, modified by Discovery Studio 2.0) show the encapsulation of substrate **4** within the pocket of the P450 BM-3 3mt (A74G F87V L188Q) protein for a) the electrostatic surface of **4** and b) the conformer for regioselective oxidation at ω -2. The α and/or β C–H bonds from the C-4 position with the fluorine substituent are not susceptible to oxidation by the high-valent iron heme center.

the corresponding substrate will be preferably oxidized to give the alcohol in the *R* configuration. However, if oxidation of the C–H_R bond involves a mechanism requiring closer interaction of the C–H bond with the activated Fe^{IV}=O, then binding of the substrate to the hydrophobic pocket must be eventually followed by a conformational change to allow hydrogen abstraction/radical rebound or direct O-atom insertion to form the product.^[7b,27] To accomplish this, according to the crystal structures of BM-3 (Figure 2), the residues Phe87 (Val87), Ala264, Thr268, and Ala328 must move to bring the C–H_R bond in closer proximity to the porphyrin with the activated oxyferryl species. If there is direct interaction between some parts of the substrate with the porphyrin system, we surmise that this conformational

switching will become more likely or facile. In any case, the stereoselectivity will reflect the orientation of the hydrocarbon in the binding pocket before conformational switching for product formation, with the enantiomeric excess determined by the free energy of orientating the substrate in the binding site. This is the kind of scenario that has been proposed for direct oxene insertion into the C–H bonds of aliphatics by the particulate methane monooxygenase (pMMO).^[10,13d,21,28]

In the case of the 3mt F328 enzyme, we have observed mainly ω -1 selectivity. To account for this behavior, we propose a specific CF₂ interaction with the Phe π system at residue 328, which must be stronger than Ala at this position in the BM-3 3mt enzyme to limit the distribution of the substrates to one major binding site. Molecular modeling reveals a possible conformer of substrate **4** that would account for the high regiospecific activation at ω -1 in the 3mt F328 (Figure 4). In this almost fully extended *all-trans* conformer,

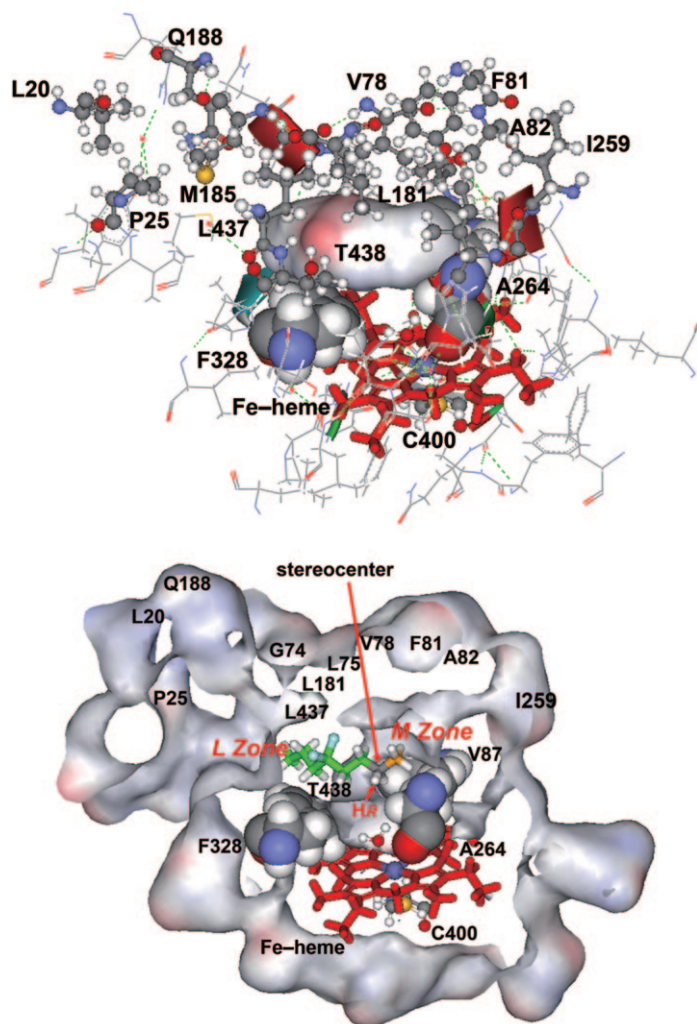


Figure 4. Three-dimensional model (PDB code 1JPZ, modified by Discovery Studio 2.0) show the encapsulation of substrate **4** within the pocket of the P450 BM-3 3mt F328 (A74G F87V L188Q A328F) protein for a) the electrostatic surface of **4** and b) the conformer for regiospecific oxidation at ω -1.

the substrate is presumably optimized for ω -1 activation by the high-valent Fe=O species of the porphyrin. Such a specific interaction would, of course, limit the activation of substrates in certain positions, such as the ω -2 and ω -3 positions.^[29]

Apparently, the mutations do not affect the protein folding dramatically or the catalytic cycle, that is, compound I is still formed and electron and proton transfers during the catalytic cycle are not affected. The dramatic difference in the product throughputs and coupling efficiencies observed between the fluorinated octanes and *n*-octane in the case of 3mt, as well as the A328F variant, suggests that the fluorinated substituent is tuning the distribution of accessible enzyme conformations and associated protein dynamics that activate the iron porphyrin for substrate hydroxylation to allow reactions mediated by the high-valent Fe=O to become kinetically more commensurate with electron transfer from the FAD/FMN reductase. In the case of the 3mt protein, given that the enhanced coupling efficiency transcends the entire set of fluorinated octanes studied, irrespective of the location of the substituent, we surmise that there must be a similar interaction involving the CF₂ group or C–F bond with the porphyrin π system (26 π electrons) that is altering the energetics and dynamics of the P450. Such an interaction would tighten up the domain of the protein containing the active site.^[30] Strong evidence for a similar CF₂... π interaction has also been demonstrated in a recent study of the binding of tumor promoters to peptide analogues of the C1B domain of the protein kinase C isozyme PKC δ , in which the replacement of Pro11 by 4,4-difluoroproline was found to exert a strong promoting effect on the binding of the teleocidins indolelactam V and naphtholactam-V8 (aromatic rings with 10 π electrons) relative to the benzolactam-V8 (6 π electrons) to the model peptide.^[31]

It is also proposed that there is a van der Waals interaction between CF₂ and the Phe π system at residue 328 when 4,4-difluorooctane is used as a substrate with BM-3 3mt A328F (Figure 1). This interaction involves polarization of the Phe π cloud by the C–F dipole moment. The polarizability of the C–F bond is quite low^[32] (molecular polarizabilities of ethane, 1-fluoroethane, and 1,1,1-trifluoroethane are 4.47, 4.96, and 4.4×10^{-24} cm³, respectively), but the dipole moment of the C–F bond is large (molecular dipole moments of CH₃F, CH₂F₂, and CHF₃ are 1.86, 1.98, and 1.65 D, respectively; the C–F bond moment is 1.4 D).^[33] The molecular polarizability of Phe is estimated to be 10 – 15×10^{-24} cm³. For comparison, the electric dipole polarizability of a methyl group is about 2.5×10^{-24} cm³.

Conclusion

In this study, we have shown that it is possible to tune the reactivity, regioselectivity, and stereoselectivity of CH activation of *n*-octanes by cytochrome P450 BM-3 with fluorine substituents. Evidence was obtained for van der Waals interactions between a CF₂ group with aromatic π systems, which

could be exploited to tune the details of the binding of the substrate to the binding pocket, as well as the protein conformational states and protein dynamics that participate in electron transfer and C–H activation.

Experimental Section

General: All chemicals were purchased from commercial sources as reagent-grade quality and were used as received unless stated otherwise. Analytical TLC was performed on precoated plates (silica gel 60 F-254) purchased from Merck. Visualization of spots on TLC was accomplished by use of KMnO_4 (aq). Mixtures of ethyl acetate and hexane were used as eluents. Purification by gravity column chromatography was carried out with EM Reagents Silica Gel 60 (particle size 0.063–0.200 mm, 70–230 mesh ASTM). NMR spectra were recorded on Bruker AVA-300 (300 MHz), AV-400 (400 MHz), or AV-800 (800 MHz) spectrophotometers. Chemical shifts (in ppm) were referenced either to the internal standard CFCl_3 (^{19}F NMR) or to the residual solvent peak (^1H and ^{13}C NMR). UV/Vis spectra were recorded on a HP 8453 diode array spectrometer or Beckman Coulter DU-800 spectrometer. HR-ESI (Waters LCT Premier XE) mass spectra were obtained with dual ionization source options and the limitation was $m/z < 1500$. Gas chromatography was performed by using an Agilent HP6890 *plus* instrument either equipped with a flame ionization detector (FID) or with a 5971 EI-MS detector and separated by a HP-1 or HP-5 capillary column (60 m \times 0.25 mm \times 0.25 μm film thickness). The analysis conditions were as follows unless stated otherwise: carrier gas, nitrogen, 1.0–2.1 mL min^{-1} ; oven temperature, 100 °C; injection port, 280 °C with a splitless ratio.

Construction of expression vector *pET21_{BM-3}*: The growth of *Bacillus megaterium* (BCRC10608 (ATCC14581), Bioresource and Collection Research Center in Hsinchu, Taiwan) was carried out by following the American Type Culture Collection culture conditions using ATCC medium3 (50 mL) in a 250 mL flask. The genomic DNA was prepared by using the Gene-Spin Genomic DNA kit (Protech, Taipei, Taiwan). The four nucleic acid primers expression of the P450 BM-3 and associated reductase genes (*BM-1af*: 5'-AATTCACAATTAAGAAATGCCTCAGCCAA-3'; *BM-1ar*: 5'-GCCAGCCCACACGTCCTTTT-3'; *BM-1bf*: 5'-CACAATTAAGAAATGCCTCAGCCAAAAA-3', and *BM-1br*: 5'-TCGAGCCCAGCCCACACG-3') were synthesized by Protech or Tri-I (Taipei, Taiwan). Together with PfuTurbo DNA polymerase (Stratagene), the P450 BM-3 gene fused with FAD/FMN reductase was amplified from genomic DNA by the polymerase chain reaction (PCR). After 5'-phosphorylation, denaturation, and renaturation of PCR products, the cohesive end, *P450_{BM-3}*, including the reductase gene with 5'-*Eco*I and 3'-*Xho*I sites was generated, and cloned into the corresponding restriction sites of *pET21a* (Novagen) to produce *pET21_{BM-3}*.

Site-directed mutagenesis of two variants of P450 BM-3 3mt (A74G F87V L188Q) and P450 BM-3 3mt F328: The mutant P450 BM-3 3mt was introduced by using a Quick-change site-directed mutagenesis kit (Stratagene) according to the manufacturer's protocol. PCR amplifications were carried out with complementary mutagenesis primers sequentially for A74G_f, 5'-GCTTTGATAAAAACTTAAGTCAAGGCCTTAAATTTGTACGTGA-3' and A74G_r, 5'-TCACGTACAAATTTAAGGCCTTGACTTAAGTTTTATCAAAGC-3', F87V_f, 5'-GCAGGAGACGGGTTAGTACAAGCTGGACGCAT-3' and F87V_r, 5'-ATGCGTCCAGCTTGTACTAACCCTGCTCCTGC-3', L188Q_f, 5'-GAAGCAATGAACAAGCAGCAGCGAGCAAATCCAGACG-3' and L188Q_r, 5'-CTGGATTTGCTCGCTGCTGCTGTT-CATGCTTCATCC-3' by using the parent plasmid *pET21_{BM-3}* as a template to create the *pET21_{BM-3}3mt* for 3mt protein expression. The vector *pET21_{BM-3}3mt_F328* for cloning of the mutant P450 BM-3 3mt F328 protein was constructed by A328F_f, 5'-CTGCGCTTATGGC-CAACTTTTCTGCGTTTCCCTATATG-3' and A328F_r, 5'-CATA-TAGGGAAAACGCAGGAAAAGTTGGCCATAAGCGCAG-3' by using *pET21_{BM-3}3mt* as the template. The mutated primer sequences, with GGC encoding for Gly, GTG for Val, CAG for Gln, and TTT for

Phe are underlined. The two variants were verified by DNA sequencing and transformed into *E. coli* BL21 (DE3) for induction and reactivity measurements.

Expression of the recombinant P450 BM-3 3mt (A74G F87V L188Q) and P450 BM-3 3mt F328 (A74G F87V L188Q A328F): Both of the vectors *pET21_{BM-3}3mt* and *pET21_{BM-3}3mt_F328* were transformed into *E. coli* BL21 (DE3). The corresponding variants were cultured in Luria-Bertani (LB) broth (100 mL) containing ampicillin (100 mg L^{-1}) at 37 °C. When the optical density of the cell culture reached 0.6–0.8 ($\text{OD}_{595}=0.6\text{--}0.8$), expression of the recombinant proteins was induced with 0.35 mM isopropyl- β -D-thiogalactoside (IPTG) at 37 °C for 6.0 h. After centrifugation at 6000 rpm, the cells were resuspended in 50 mM Tris-HCl buffer (pH 7.5) for further reactivity measurements or protein characterization. After cell lysis, we examined the expression of P450 BM-3 protein variants by 10% sodium dodecyl sulfate polyacrylamide gel electrophoresis (SDS-PAGE). The P450 BM-3 protein fused with the reductase and 6-His tags appeared on the SDS-PAGE gel at a molecular weight of about 119 kDa.

Purification of P450 BM-3 3mt and 3mt F328: Growth of *E. coli* BL21 (DE3; 600 mL; $\text{OD}_{595} \approx 0.6\text{--}0.8$) containing vectors for the expression of BM-3 variants in LB medium, supplied with ampicillin (100 mg L^{-1}) and 0.5% glucose, were induced with 0.35 mM IPTG for 6.0 h. After centrifugation at 8000 rpm (20 min, 4 °C), the cell pellet was resuspended in loading buffer (0.1 M, Tris-HCl, pH 8.2, 1 mM phenylmethanesulfonyl fluoride (PMSF)) and lysed by French press on ice (20000 psi, SLM-AMINCO Instruments). After the lysate was subjected to ultracentrifugation at 36000 rpm for 1.0 h (4 °C), the supernatant was filtered through a 0.22 μm filter, then reloaded onto a pre-equilibrated 1 mL HisTrap HP column (GE Healthcare). The column was subsequently washed with loading buffer, washing buffer A (50 mM NaH_2PO_4 , 300 mM NaCl, pH 8.0), and washing buffer B (100 mM imidazole, 50 mM NaH_2PO_4 , 300 mM NaCl, pH 8.0). The purified protein was desalting with PD-10, and finally, supplemented with 10% glycerol and stored at –80 °C. Concentrations of P450 enzymes were measured by CO difference spectroscopy of the reduced heme by using an extinction coefficient of 91 $\text{mm}^{-1} \text{cm}^{-1}$ for the 450 minus 490 nm signal.^[9b,34]

Hydroxylation of the fluorinated octane derivatives by whole-cell catalysis mediated by *E. coli* P450 BM-3 3mt and *E. coli* BM-3 3mt F328: A culture of the recombinant *E. coli* containing P450 BM-3 3mt and BM-3 3mt F328, including cofactors, were cultured in LB medium (100 mL) to $\text{OD}_{595}=0.6\text{--}0.8$ and then induced with 0.35 mM IPTG at 37 °C for 6.0 h. After centrifugation at 8000 rpm, cells were resuspended to a density corresponding to $\text{OD}_{595}=15$ with 50 mM LB buffer containing 0.5% glucose. Substrates 1–7 (1.0 μL) were then added into reaction mixtures (1 mL), and incubated at 37 °C at 170 rpm for 22 h. The reactions were then quenched and the mixtures were extracted immediately for product analysis with dichloromethane (1.0 mL). The organic layers were separated by centrifugation at 12000 rpm, and monitored by GC or GC/MSD. Finally, the alcohols obtained, **1a–d**, **2a–c**, **3a**, **3b**, **4a**, **5a–d**, **6a–c**, and **7a–c**, were separated by gravity column chromatography (EtOAc in hexane=20%) and the pure secondary alcohols were analyzed by ^{13}C , ^{19}F , and ^1H NMR spectroscopy.

Compound 1a: $R_f=0.510$ (EtOAc/hexane 1:4); GC (isothermal, 100 °C): $t_R=8.18$ min; ^1H NMR (400 MHz, CDCl_3): $\delta=5.77$ (tt, $^2J(\text{H,F})=57.2$, $^3J(\text{H,H})=4.0$ Hz, 1H; CHF_2), 3.75 (sextet, $^3J(\text{H,H})=5.6$ Hz, 1H; CHOH), 1.81–1.68 (m, 2H; CH_2), 1.50–1.28 (m, 8H; CH_2), 1.16 ppm (d, $^3J(\text{H,H})=6.0$ Hz, 3H, CH_3); ^{13}C NMR (100 MHz, CDCl_3): $\delta=117.4$ (t, $^1J(\text{C,F})=238.0$ Hz; CHF_2), 68.0 (s; CHOH), 39.0 (s; CH_2), 34.0 (t, $^2J(\text{C,F})=21.0$ Hz; CCHF_2), 29.0 (s; CH_2), 25.5 (s; CH_2), 23.5 (s; CH_3), 22.0 ppm (t, $^3J(\text{C,F})=5.0$ Hz; CCH_2CHF_2); ^{19}F NMR (282 MHz, CDCl_3): $\delta=-115.90$ ppm; EI-MS: m/z (%): 151 (2) [$M-\text{CH}_3$] $^+$, 148 (1) [$M-\text{H}_2\text{O}$] $^+$, 131 (0.5), 113 (2), 93 (0.3), 87 (2), 73 (2), 67 (5), 45 (100); HRMS (ESI) [$M+\text{Na}$] $^+$: m/z calcd for $\text{C}_8\text{H}_{16}\text{F}_2\text{O}_n\text{Na}$: 189.1067; found: 189.1065.

Compound 1b: $R_f=0.520$ (EtOAc/hexane 1:4); GC (isothermal, 100 °C): $t_R=8.02$ min; ^1H NMR (400 MHz, CDCl_3): $\delta=5.77$ (tt, $^2J(\text{H,F})=57.2$, $^3J(\text{H,H})=4.0$ Hz, 1H; CHF_2), 3.51 (m, 1H; CHOH), 1.78–1.63 (m, 2H; CH_2), 1.52–1.33 (m, 8H; CH_2), 0.92 ppm (t, $^3J(\text{H,H})=7.2$ Hz, 3H; CH_3); ^{13}C NMR (100 MHz, CDCl_3): $\delta=117.3$ (t, $^1J(\text{C,F})=237.0$ Hz; CHF_2),

72.9 (s; CHOH), 36.5 (s; CH₂), 34.0 (t, ²J(C,F)=21.0 Hz; CCF₂), 30.1 (s; CH₃), 25.1 (s; CH₂), 22.1 (t, ³J(C,F)=5.0 Hz; CCH₂CHF₂), 9.7 ppm (s; CH₃); ¹⁹F NMR (282 MHz, CDCl₃): δ = -115.86 ppm; EI-MS: *m/z* (%): 165 (0.1) [M-H]⁺, 148 (0.2) [M-H₂O]⁺, 137 (13) [M-C₂H₅]⁺, 117 (3), 99 (21), 79 (16), 73 (7), 59 (100), 41 (31); HRMS (ESI) [M+Na]⁺: *m/z* calcd for C₈H₁₆F₂O₂Na: 189.1067; found: 189.1066.

Compound 1c: *R*_f=0.530 (EtOAc/hexane 1:4); GC (isothermal, 100 °C): *t*_R=7.78 min; ¹H NMR (400 MHz, CDCl₃): δ = 5.78 (tt, ²J(H,F)=56.8, ³J(H,H)=4.4 Hz, 1H; CHF₂), 3.61 (m, 1H; CHOH), 1.91–1.79 (m, 2H; CH₂), 1.54–1.29 (m, 8H; CH₂), 0.90 ppm (t, ³J(H,H)=7.6 Hz, 3H; CH₃); ¹³C NMR (100 MHz, CDCl₃): δ = 117.3 (t, ¹J(C,F)=237.0 Hz; CHF₂), 71.2 (s; CHOH), 39.6 (s; CH₂), 36.6 (s; CH₂), 34.0 (t, ²J(C,F)=21.0 Hz; CCF₂), 18.7 (s; CH₂), 18.3 (t, ³J(C,F)=5.0 Hz; CCH₂CHF₂), 13.9 ppm (s; CH₃); ¹⁹F NMR (282 MHz, CDCl₃): δ = -115.90 ppm; EI-MS: *m/z* (%): 123 (16) [M-C₃H₇]⁺, 103 (0.9), 83 (2), 73 (46), 55 (100), 43 (28); HRMS (ESI) [M+Na]⁺: *m/z* calcd for C₈H₁₆F₂O Na: 189.1067; found: 189.1065.

Compound 1d: *R*_f=0.535 (EtOAc/hexane 1:4); GC (isothermal, 100 °C): *t*_R=7.64 min; ¹H NMR (400 MHz, CDCl₃): δ = 5.84 (tt, ²J(H,F)=56.8, ³J(H,H)=4.4 Hz, 1H; CHF₂), 3.60 (m, 1H; CHOH), 1.99–1.90 (m, 2H; CH₂), 1.65–1.56 (m, 2H; CH₂), 1.54–1.29 (m, 6H; CH₂), 0.90 ppm (t, ³J(H,H)=7.6 Hz, 3H; CH₃); ¹³C NMR (75 MHz, CDCl₃): δ = 117.4 (t, ¹J(C,F)=237.0 Hz; CHF₂), 71.1 (s; CHOH), 37.3 (s; CH₂), 30.5 (t, ²J(C,F)=21.0 Hz; CCF₂), 29.4 (t, ³J(C,F)=5.3 Hz; CCH₂CHF₂), 27.7 (s; CH₂), 22.6 (s; CH₂), 13.99 ppm (s; CH₃); ¹⁹F NMR (282 MHz, CDCl₃): δ = -115.88, -116.14 ppm; EI-MS: *m/z* (%): 109 (47) [M-C₄H₉]⁺, 89 (47), 87 (46), 71 (3), 69 (100), 51 (13), 41 (92); HRMS (ESI) [M+Na]⁺: *m/z* calcd for C₈H₁₆F₂O₂Na: 189.1067; found: 189.1072.

Compound 2a: *R*_f=0.520 (EtOAc/hexane 1:4); GC (isothermal, 100 °C): *t*_R=7.12 min; ¹H NMR (400 MHz, CDCl₃): δ = 3.77 (sextet, ³J(H,H)=8.0 Hz, 1H; CHOH), 1.87–1.75 (m, 2H; CH₂), 1.55 (t, ³J(H,F)=6.0 Hz, 3H; CH₃CF₂), 1.47–1.31 (m, 6H; CH₂), 1.17 ppm (d, ³J(H,H)=4.0 Hz, 3H; CH₃); ¹³C NMR (100 MHz, CDCl₃): δ = 124.3 (t, ¹J(C,F)=236.0 Hz; CF₂), 67.9 (s; CHOH), 38.9 (s; CH₂), 37.9 (t, ²J(C,F)=24.8 Hz; CCF₂), 25.4 (s; CH₂), 23.5 (s; CH₃), 23.2 (t, ²J(C,F)=24.8 Hz; CCF₂), 22.8 ppm (t, ³J(C,F)=4.5 Hz; CCH₂CF₂); ¹⁹F NMR (282 MHz, CDCl₃): δ = -90.62 ppm; EI-MS: *m/z* (%): 151 (0.5) [M-CH₃]⁺, 131 (1) [M-CH₃-HF]⁺, 113 (21), 102 (14), 93 (5), 82 (16), 73 (54), 45 (100); HRMS (ESI) [M+Na]⁺: *m/z* calcd for C₈H₁₆F₂O₂Na: 189.1067; found: 189.1065.

Compound 2b: *R*_f=0.530 (EtOAc/hexane 1:4); GC (isothermal, 100 °C): *t*_R=6.93 min; ¹H NMR (400 MHz, CDCl₃): δ = 3.54–3.48 (1H, m, CHOH), 1.89–1.77 (m, 4H; CH₂), 1.58 (t, ³J(H,F)=16.0 Hz, 3H; CH₃CF₂), 1.49–1.38 (m, 4H; CH₂), 0.92 ppm (t, ³J(H,H)=7.6 Hz, 3H; CH₃); ¹³C NMR (100 MHz, CDCl₃): δ = 124.3 (t, ¹J(C,F)=237.0 Hz; CF₂), 73.0 (s; CHOH), 37.9 (t, ²J(C,F)=25.5 Hz; CCF₂), 36.4 (s; CH₂), 30.2 (s; CH₂), 23.2 (t, ²J(C,F)=28.5 Hz; CCF₂), 19.0 (t, ³J(C,F)=6.0 Hz; CCH₂CF₂), 9.8 ppm (s; CH₃); ¹⁹F NMR (282 MHz, CDCl₃): δ = -90.55 ppm; EI-MS: *m/z* (%): 137 (1) [M-C₂H₅]⁺, 117 (22), 99 (48), 73 (77), 59 (100), 41 (30); HRMS (ESI) [M+Na]⁺: *m/z* calcd for C₈H₁₆F₂O₂Na: 189.1067; found: 189.1067.

Compound 2c: *R*_f=0.540 (EtOAc/hexane 1:4); GC (isothermal, 100 °C): *t*_R=6.61 min; ¹H NMR (400 MHz, CDCl₃): δ = 3.64–3.58 (m, 1H; CHOH), 1.71–1.52 (m, 4H; CH₂), 1.55 (t, ³J(H,F)=18.0 Hz, 3H; CH₃CF₂), 1.48–1.41 (m, 4H; CH₂), 0.92 ppm (t, ³J(H,H)=7.2 Hz, 3H; CH₃); ¹³C NMR (100 MHz, CDCl₃): δ = 124.4 (t, ¹J(C,F)=235.0 Hz; CF₂), 71.0 (s; CHOH), 39.7 (s; CH₂), 34.1 (t, ²J(C,F)=25.0 Hz; CCF₂), 30.2 (s; CH₂), 23.4 (t, ²J(C,F)=25.0 Hz; CCF₂), 18.8 (s; CH₂), 14.0 ppm (s; CH₃); ¹⁹F NMR (282 MHz, CDCl₃): δ = -90.92, -91.28 ppm; EI-MS: *m/z* (%): 123 (10) [M-C₃H₇]⁺, 103 (67), 83 (18), 73 (56), 65 (20), 55 (100), 43 (35), 29 (17); HRMS (ESI) [M+Na]⁺: *m/z* calcd for C₈H₁₆F₂O₂Na: 189.1067; found: 189.1068.

Compound 3a: *R*_f=0.520 (EtOAc/hexane 1:4); GC (isothermal, 100 °C): *t*_R=7.37 min; ¹H NMR (300 MHz, CDCl₃): δ = 3.79 (sextet, ³J(H,H)=6.0 Hz, 1H; CHOH), 1.91–1.72 (m, 6H; CH₂), 1.61–1.35 (m, 2H; CH₂), 1.17 (d, ³J(H,H)=6.3 Hz, 3H; CH₃), 0.98 ppm (t, ³J(H,H)=7.5 Hz, 3H; CH₃); ¹³C NMR (75 MHz, CDCl₃): δ = 125.4 (t, ¹J(C,F)=239.0 Hz; CF₂), 67.8 (s; CHOH), 38.8 (s; CH₂), 35.8 (t, ²J(C,F)=26.0 Hz; CCF₂), 29.5 (t, ²J(C,F)=26.0 Hz; CCF₂), 23.5 (s; CH₂), 18.6 (s; CH₃), 6.6 ppm (t, ³J(C,F)=5.3 Hz; CCH₂CF₂); ¹⁹F NMR (282 MHz, CDCl₃): δ = -100.21 ppm; EI-MS: *m/z* (%): 151 (1) [M-CH₃]⁺, 131 (2) [M-CH₃-HF]⁺, 113 (7), 102 (16), 87 (21), 74 (100), 59 (27), 45 (78); HRMS (ESI) [M+Na]⁺: *m/z* calcd for C₈H₁₆F₂O₂Na: 189.1067; found: 189.1063.

Compound 3b: *R*_f=0.530 (EtOAc/hexane 1:4); GC (isothermal, 100 °C): *t*_R=7.06 min; ¹H NMR (300 MHz, CDCl₃): δ = 3.56–3.48 (m, 1H; CHOH), 1.97–1.62 (m, 4H; CH₂), 1.60–1.36 (m, 4H; CH₂), 0.98 (t, ³J(H,H)=7.5 Hz, 3H; CH₃), 0.92 ppm (t, ³J(H,H)=7.5 Hz, 3H; CH₃); ¹³C NMR (75 MHz, CDCl₃): δ = 125.6 (t, ¹J(C,F)=239.0 Hz; CF₂), 72.7 (s; CHOH), 32.0 (t, ²J(C,F)=26.0 Hz; CCF₂), 30.3 (s; CH₂), 29.7 (t, ²J(C,F)=26.0 Hz; CCF₂), 29.3 (t, ³J(C,F)=4.5 Hz; CCH₂CF₂), 9.8 (s; CH₃), 6.6 ppm (t, ³J(C,F)=6.0 Hz; CCH₂CF₂); ¹⁹F NMR (282 MHz, CDCl₃): δ = -100.50, -100.61 ppm; EI-MS: *m/z* (%): 137 (4) [M-C₂H₅]⁺, 117 (64) [M-C₂H₅-HF]⁺, 99 (12), 88 (46), 79 (11), 69 (51), 59 (100), 41 (36); HRMS (ESI) [M+Na]⁺: *m/z* calcd for C₈H₁₆F₂O₂Na: 189.1067; found: 189.1064.

Compound 4a: *R*_f=0.530 (EtOAc/hexane 1:4); GC (isothermal, 100 °C): *t*_R=7.01 min; ¹H NMR (400 MHz, CDCl₃): δ = 3.81 (sextet, ³J(H,H)=6.4 Hz, 1H; CHOH), 2.02–1.45 (m, 8H; CH₂), 1.21 (d, ³J(H,H)=6.0 Hz, 3H; CH₃), 0.94 ppm (t, ³J(H,H)=7.2 Hz, 3H; CH₃); ¹³C NMR (100 MHz, CDCl₃): δ = 125.2 (t, ¹J(C,F)=238.0 Hz; CF₂), 67.5 (s; CHOH), 38.6 (t, ²J(C,F)=25.0 Hz; CCF₂), 32.5 (t, ²J(C,F)=25.0 Hz; CCF₂), 31.6 (s; CH₂), 23.6 (s; CH₂), 15.8 (t, ³J(C,F)=4.0 Hz; CCH₂CF₂), 13.9 ppm (s; CH₃); ¹⁹F NMR (282 MHz, CDCl₃): δ = -98.17, -98.25 ppm; EI-MS: *m/z* (%): 151 (0.6) [M-CH₃]⁺, 131 (21) [M-CH₃-HF]⁺, 113 (4), 102 (83), 93 (1), 87 (18), 74 (100), 67 (11), 59 (15), 41 (16); HRMS (ESI) [M+Na]⁺: *m/z* calcd for C₈H₁₆F₂O₂Na: 189.1067; found: 189.1065.

Compound 5a: *R*_f=0.540 (EtOAc/hexane 1:4); GC (isothermal, 100 °C): *t*_R=9.03 min; ¹H NMR (300 MHz, CDCl₃): δ = 4.42 (dt, ²J(H,F)=45.0 and ³J(H,H)=6.0 Hz, 2H; CH₂F), 3.77 (sextet, ³J(H,H)=4.5 Hz, 1H; CHOH), 1.74–1.61 (m, 2H; CH₂), 1.43–1.33 (m, 8H; CH₂), 1.28 ppm (d, ³J(H,H)=6.0 Hz, 3H; CH₃); ¹³C NMR (75 MHz, CDCl₃): δ = 84.1 (d, ¹J(C,F)=164.0 Hz; CH₂F), 68.1 (s; CHOH), 39.1 (s; CH₂), 30.3 (d, ²J(C,F)=19.5 Hz; CCH₂F), 29.2 (s; CH₂), 25.6 (s; CH₂), 25.1 (d, ³J(C,F)=5.3 Hz; CCH₂CH₂F), 23.4 ppm (s; CH₂); ¹⁹F NMR (282 MHz, CDCl₃): δ = -218.16 ppm; EI-MS: *m/z* (%): 133 (0.5) [M-CH₃]⁺, 130 (1) [M-H₂O]⁺, 95 (9), 69 (1), 55 (16), 45 (100), 41 (22); HRMS (ESI) [M+Na]⁺: *m/z* calcd for C₈H₁₇FONa: 171.1161; found: 171.1167.

Compound 5b: *R*_f=0.550 (EtOAc/hexane 1:4); GC (isothermal, 100 °C): *t*_R=8.87 min; EI-MS: *m/z* (%): 130 (0.6) [M-H₂O]⁺, 119 (9) [M-C₂H₅]⁺, 101 (1), 99 (1), 81 (47), 59 (100), 55 (41), 41 (33), 31 (26).

Compound 5c: *R*_f=0.550 (EtOAc/hexane 1:4); GC (isothermal, 100 °C): *t*_R=8.58 min; EI-MS: *m/z* (%): 130 (0.6) [M-H₂O]⁺, 105 (21) [M-C₃H₇]⁺, 85 (18), 73 (58), 67 (23), 55 (100), 41 (5), 29 (29).

Compound 5d: *R*_f=0.550 (EtOAc/hexane 1:4); GC (isothermal, 100 °C): *t*_R=8.42 min; EI-MS: *m/z* (%): 130 (1) [M-H₂O]⁺, 91 (57), 87 (35), 71 (69), 69 (100), 55 (15).

Compound 6a: *R*_f=0.540 (EtOAc/hexane 1:4); GC (isothermal, 100 °C): *t*_R=14.78 min; ¹⁹F NMR (282 MHz, CDCl₃): δ = -218.29, -228.37; EI-MS: *m/z* (%): 133 (4) [M-CH₂F]⁺, 95 (100), 69 (42), 63 (22), 55 (49), 47 (10), 45 (14), 41 (65), 33 (10).

Compound 6b: *R*_f=0.535 (EtOAc/hexane 1:4); GC (isothermal, 100 °C): *t*_R=16.52 min; ¹H NMR (300 MHz, CDCl₃): δ = 4.71–4.05 (m, 2H; CH₂), 4.39 (dt, ²J(H,F)=47.1 and ³J(H,H)=6.0 Hz, 2H; CH₂F), 3.80–3.72 (m, 1H; CHOH), 1.92–1.56 (m, 6H; CH₂), 1.47–1.28 ppm (m, 4H; CH₂); ¹³C NMR (75 MHz, CDCl₃): δ = 84.0 (d, ¹J(C,F)=163.0 Hz; CH₂F), 81.7 (d, ¹J(C,F)=163.0 Hz; CH₂F), 68.3 (d, ³J(C,F)=5.0 Hz; CFH₂CH₂COH), 37.6 (d, ²J(C,F)=19.0 Hz; CCH₂F), 37.4 (s; CH₂), 30.2 (d, ²J(C,F)=20.0 Hz; CCH₂F), 25.1 ppm (s; CH₂); ¹⁹F NMR (282 MHz, CDCl₃): δ = -218.29, -220.67 ppm; EI-MS: *m/z* (%): 119 (16) [M-C₂H₅F]⁺, 99 (2), 81 (70), 77 (22), 55 (65), 47 (16), 41 (43), 33 (8); HRMS (ESI) [M+Na]⁺: *m/z* calcd for C₈H₁₆F₂O₂Na: 189.1067; found: 189.1070.

Compound 6c: *R*_f=0.530 (EtOAc/hexane 1:4); GC (isothermal, 100 °C): *t*_R=17.36 min; ¹H NMR (400 MHz, CDCl₃): δ = 4.45 (dt, ²J(H,F)=47.2, ³J(H,H)=5.6 Hz, 2H; CH₂F), 4.42 (dt, ²J(H,F)=47.2 and ³J(H,H)=6.0 Hz, 2H; CH₂F), 3.64–3.58 (m, 1H; CHOH), 1.92–1.42 ppm (m, 10H,

CH₂); ¹³C NMR (100 MHz, CDCl₃): δ = 84.1 (d, ¹J(C,F) = 163.0 Hz; CH₂F), 83.9 (d, ¹J(C,F) = 163.0 Hz; CH₂F), 71.2 (s; CHO), 37.0 (s; CH₂), 33.0 (d, ²J(C,F) = 4.0 Hz; CCH₂CH₂F), 30.3 (d, ²J(C,F) = 20.0 Hz; CCH₂F), 26.7 (d, ²J(C,F) = 20.0 Hz; CCH₂F), 21.4 ppm (d, ³J(C,F) = 5.0 Hz; CCH₂CH₂F); ¹⁹F NMR (282 MHz, CDCl₃): δ = -217.92, -218.44 ppm; EI-MS: *m/z* (%): 105 (25) [M–C₃H₅F]⁺, 91 (64) [M–C₄H₈F]⁺, 85 (18), 81 (2), 71 (49), 67 (30), 61 (5), 55 (27), 53 (6), 47 (9); HRMS (ESI) [M+Na]⁺: *m/z* calcd for C₈H₁₆F₂O₄Na: 189.1067; found: 189.1071.

Compound 7a: *R*_f = 0.530 (EtOAc/hexane 1:4); GC (isothermal, 100 °C): *t*_R = 7.50 min; EI-MS: *m/z* (%): 183 (0.2) [M–H]⁺, 169 (2) [M–CH₃]⁺, 166 (1) [M–H₂O]⁺, 151 (2), 131 (1), 105 (0.5), 91 (1), 77 (4), 45 (100).

Compound 7b: *R*_f = 0.530 (EtOAc/hexane 1:4); GC (isothermal, 100 °C): *t*_R = 7.34 min; EI-MS: *m/z* (%): 183 (0.2) [M–H]⁺, 166 (0.4) [M–H₂O]⁺, 155 (13) [M–C₂H₅]⁺, 137 (5), 117 (10), 97 (5), 59 (100), 41 (21).

Compound 7c: *R*_f = 0.530 (EtOAc/hexane 1:4); GC (isothermal, 100 °C): *t*_R = 7.22 min; EI-MS: *m/z* (%): 166 (0.2) [M–H₂O]⁺, 141 (19) [M–C₃H₇]⁺, 121 (33), 101 (0.8), 83 (2), 73 (67), 57 (9), 55 (100), 43 (31).

Preparation of 1a'–5a', 1b'–3b' and 5b: (*R*)-*O*-Acetylmandelic acid (76 mg, 0.39 mmol, 1.3 equiv) and DMAP (4.0 mg) were dissolved in dichloromethane (5.0 mL) at -40 °C in a 10 mL round-bottomed flask. Over the next 5 min, a solution of DCC (75 mg, 0.39 mmol, 1.3 equiv) in dichloromethane (5.0 mL) was added dropwise to the flask. A white precipitate resulted after 10 min. Then, a solution of authentic standards of the octanol stereoisomers or fluorinated alcoholic products (0.30 mmol, 1.0 equiv) in dichloromethane (1.0 mL) was added over a second 5 min period, and the mixture was stirred overnight at room temperature. The suspension was filtered through a pad of silica gel and washed with dichloromethane (5–10 mL). The filtrate was evaporated to near dryness under vacuum and the residue was suspended in dichloromethane (ca. 2.0 mL). The corresponding products were further purified by gravity column chromatography (EtOAc in hexane = 20%) and analyzed by ¹³C and ¹H NMR spectroscopy and GC/MSD.

Compound (R)-1a': *R*_f = 0.89 (EtOAc/hexane 1:4); GC (isothermal, 140 °C; flow rate: 0.8 mL min⁻¹): *t*_R = 214 min; ¹H NMR (300 MHz, CDCl₃): δ = 7.46–7.43 (m, 2H; Ar-H), 7.37–7.34 (m, 3H; Ar-H), 5.84 (s, 1H; PhCHOCO), 5.70 (tt, ²J(H,F) = 57.0, ³J(H,H) = 4.5 Hz, 1H; CHF₂), 4.98–4.82 (m, 1H; CH₃CHOCO), 1.78–1.05 (m, 10H; CH₂), 1.22 ppm (d, ³J(H,H) = 6.0 Hz, 3H; CH₃); ¹⁹F NMR (282 MHz, CDCl₃): δ = -115.93, -115.89 ppm; EI-MS: *m/z* (%): 177 (3); 149 (59); 135 (2); 118 (4); 107 (100); 43 (44); 28 (15); HRMS (ESI) [M+Na]⁺: *m/z* calcd for C₁₈H₂₅FO₄Na: 365.1540; found: 365.1537.

Compound (S)-1a': *R*_f = 0.89 (EtOAc/hexane 1:4); GC (isothermal, 140 °C; flow rate: 0.8 mL min⁻¹): *t*_R = 216 min; ¹H NMR (300 MHz, CDCl₃): δ = 7.46–7.43 (m, 2H; Ar-H), 7.37–7.34 (m, 3H; Ar-H), 5.83 (s, 1H; PhCHOCO), 5.76 (tt, ²J(H,F) = 57.0, ³J(H,H) = 4.5 Hz, 1H; CHF₂), 4.98–4.82 (m, 1H; CH₃CHOCO), 1.78–1.05 (m, 10H; CH₂), 1.04 ppm (d, ³J(H,H) = 6.0 Hz, 3H; CH₃); ¹⁹F NMR (282 MHz, CDCl₃): δ = -115.93, -115.89 ppm; EI-MS: *m/z* (%): 177 (3); 149 (59); 135 (2); 118 (4); 107 (100); 43 (44); 28 (15); HRMS (ESI) [M+Na]⁺: *m/z* calcd for C₁₈H₂₅FO₄Na: 365.1540; found: 365.1537.

Compound (R)-1b': *R*_f = 0.90 (EtOAc/hexane 1:4); GC (isothermal, 140 °C; flow rate: 0.8 mL min⁻¹): *t*_R = 192 min; EI-MS: *m/z* (%): 177(3); 149 (59); 135 (2); 118 (4); 107 (100); 43 (44); 28 (15).

Compound (S)-1b': *R*_f = 0.90 (EtOAc/hexane 1:4); GC (isothermal, 140 °C; flow rate: 0.8 mL min⁻¹): *t*_R = 195 min; EI-MS: *m/z* (%): 177(3); 149 (59); 135 (2); 118 (4); 107 (100); 43 (44); 28 (15).

Compound (R)-2a': *R*_f = 0.89 (EtOAc/hexane 1:4); GC (isothermal, 140 °C; flow rate: 0.8 mL min⁻¹): *t*_R = 185 min; ¹H NMR (400 MHz, CDCl₃): δ = 7.45–7.43 (m, 2H; Ar-H), 7.36–7.33 (m, 3H; Ar-H), 5.85 (s, 1H; PhCHOCO), 4.96–4.86 (m, 1H; CHOCO), 2.17 (s, 3H; CH₃CO), 1.64–1.52 (m, 2H; CF₂CH₂), 1.49 (t, ³J(H,F) = 15.0 Hz, 3H; CH₃CF₂), 1.46–1.37 (m, 6H; CH₂), 1.22 ppm (d, ³J(H,H) = 6.0 Hz, 3H; CH₃); ¹⁹F NMR (282 MHz, CDCl₃): δ = -90.60 ppm; EI-MS: *m/z* (%): 177 (3); 149 (59); 135 (2); 118 (4); 107 (100); 43 (44); 28 (15); HRMS (ESI) [M+Na]⁺: *m/z* calcd for C₁₈H₂₄F₂O₄Na: 365.1540; found: 365.1536.

Compound (S)-2a': *R*_f = 0.89 (EtOAc/hexane 1:4); GC (isothermal, 140 °C; flow rate: 0.8 mL min⁻¹): *t*_R = 187 min; ¹H NMR (400 MHz, CDCl₃): δ = 7.45–7.43 (m, 2H; Ar-H), 7.36–7.33 (m, 3H; Ar-H), 5.83 (s, 1H; PhCHOCO), 4.96–4.86 (m, 1H; CHOCO), 2.17 (s, 3H; CH₃CO), 1.64–1.52 (m, 2H; CH₃CF₂CH₂), 1.49 (t, ³J(H, F) = 15.0 Hz, 3H; CH₃CF₂), 1.46–1.37 (m, 4H; CH₂), 1.05 (d, ³J(H,H) = 6.0 Hz, 3H; CH₃), 1.10–0.93 ppm (m, 2H; CH₂); ¹⁹F NMR (282 MHz, CDCl₃): δ = -90.60 ppm; EI-MS: *m/z* (%): 177(3); 149 (59); 135 (2); 118 (4); 107 (100); 43 (44); 28 (15); HRMS (ESI) [M+Na]⁺: *m/z* calcd for C₁₈H₂₄F₂O₄Na: 365.1540; found: 365.1536.

Compound (R)-2b': *R*_f = 0.90 (EtOAc/hexane 1:4); GC (isothermal, 140 °C; flow rate: 0.8 mL min⁻¹): *t*_R = 164 min; ¹H NMR (400 MHz, CDCl₃): δ = 7.47–7.43 (m, 2H; Ar-H), 7.37–7.33 (m, 3H; Ar-H), 5.85 (s, 1H; PhCHOCO), 4.87–4.78 (m, 1H; CHOCO), 2.17 (s, 3H; CH₃CO), 1.67–1.38 (m, 6H; CH₂), 1.38 (t, ³J(H,F) = 21.0 Hz, 3H; CH₃CF₂), 1.15–1.04 (m, 2H; CH₂), 0.88 ppm (t, ³J(H,H) = 6.0 Hz, 3H; CH₃); ¹⁹F NMR (282 MHz, CDCl₃): δ = -90.38, -90.49 ppm; EI-MS: *m/z* (%): 177 (3); 149 (59); 135 (2); 118 (4); 107 (100); 43 (44); 28 (15); HRMS (ESI) [M+Na]⁺: *m/z* calcd for C₁₈H₂₄F₂O₄Na: 365.1540; found: 365.1548.

Compound (S)-2b': *R*_f = 0.90 (EtOAc/hexane 1:4); GC (isothermal, 140 °C; flow rate: 0.8 mL min⁻¹): *t*_R = 166 min; ¹H NMR (400 MHz, CDCl₃): δ = 7.47–7.43 (m, 2H; Ar-H), 7.37–7.33 (m, 3H; Ar-H), 5.84 (s, 1H; PhCHOCO), 4.87–4.78 (m, 1H; CHOCO), 2.17 (s, 3H; CH₃CO), 1.67–1.38 (m, 6H; CH₂), 1.38 (t, ³J(H,F) = 21.0 Hz, 3H; CH₃CF₂), 1.15–1.04 (m, 2H; CH₂), 0.57 ppm (t, ³J(H,H) = 6.0 Hz, 3H; CH₃); ¹⁹F NMR (282 MHz, CDCl₃): δ = -90.38, -90.49 ppm; EI-MS: *m/z* (%): 177 (3); 149 (59); 135 (2); 118 (4); 107 (100); 43 (44); 28 (15); HRMS (ESI) [M+Na]⁺: *m/z* calcd for C₁₈H₂₄F₂O₄Na: 365.1540; found: 365.1548.

Compound (R)-2c': *R*_f = 0.91 (EtOAc/hexane 1:4); GC (isothermal, 140 °C; flow rate: 0.8 mL min⁻¹): *t*_R = 139 min; ¹H NMR (400 MHz, CDCl₃): δ = 7.48–7.44 (m, 2H; Ar-H), 7.38–7.34 (m, 3H; Ar-H), 5.84 (s, 1H; PhCHOCO), 4.91–4.88 (m, 1H; CHOCO), 2.18 (s, 3H; CH₃CO), 1.62–1.42 (m, 4H; CH₂), 1.32 (t, ³J(H,H) = 18.0 Hz, 3H; CH₃CF₂), 1.40–1.21 (m, 4H; CH₂), 0.89 ppm (t, ³J(H,H) = 6.0 Hz, 3H; CH₃); ¹⁹F NMR (282 MHz, CDCl₃): δ = -92.33, -92.42 ppm; EI-MS: *m/z* (%): 177 (3); 149 (59); 135 (2); 118 (4); 107 (100); 43 (44); 28 (15); HRMS (ESI) [M+Na]⁺: *m/z* calcd for C₁₈H₂₄F₂O₄Na: 365.1540; found: 365.1544.

Compound (S)-2c': *R*_f = 0.91 (EtOAc/hexane 1:4); GC (isothermal, 140 °C; flow rate: 0.8 mL min⁻¹): *t*_R = 139 min; ¹H NMR (400 MHz, CDCl₃): δ = 7.48–7.44 (m, 2H; Ar-H), 7.38–7.34 (m, 3H; Ar-H), 5.82 (s, 1H; PhCHOCO), 4.91–4.88 (m, 1H; CHOCO), 2.18 (s, 3H; CH₃CO), 1.62–1.42 (m, 4H; CH₂), 1.32 (t, ³J(H,H) = 18.0 Hz, 3H; CH₃CF₂), 1.40–1.21 (m, 4H; CH₂), 0.69 ppm (t, ³J(H,H) = 6.0 Hz, 3H; CH₃); ¹⁹F NMR (282 MHz, CDCl₃): δ = -92.33, -92.42 ppm; EI-MS: *m/z* (%): 177 (3); 149 (59); 135 (2); 118 (4); 107 (100); 43 (44); 28 (15); HRMS (ESI) [M+Na]⁺: *m/z* calcd for C₁₈H₂₄F₂O₄Na: 365.1540; found: 365.1544.

Compound (R)-3a': *R*_f = 0.89 (EtOAc/hexane 1:4); GC (isothermal, 130 °C; flow rate: 0.5 mL min⁻¹): *t*_R = 412 min; ¹H NMR (300 MHz, CDCl₃): δ = 7.46–7.42 (m, 2H; Ar-H), 7.38–7.33 (m, 3H; Ar-H), 5.85 (s, 1H; PhCHOCO), 4.98–4.86 (m, 1H; CH₃CHOCO), 2.17 (s, 3H; CH₃CO), 1.81–1.37 (m, 8H; CH₂), 1.24 (d, ³J(H,H) = 6.0 Hz, 3H; CH₃), 0.90 ppm (t, ³J(H,H) = 7.5 Hz, 3H; CH₃); ¹⁹F NMR (282 MHz, CDCl₃): δ = -100.22 ppm; EI-MS: *m/z* (%): 177 (3); 149 (59); 135 (2); 118 (4); 107 (100); 43 (44); 28 (15); HRMS (ESI) [M+Na]⁺: *m/z* calcd for C₁₈H₂₄F₂O₄Na: 365.1540; found: 365.1547.

Compound (S)-3a': *R*_f = 0.89 (EtOAc/hexane 1:4); GC (isothermal, 130 °C; flow rate: 0.5 mL min⁻¹): *t*_R = 414 min; ¹H NMR (300 MHz, CDCl₃): δ = 7.46–7.42 (m, 2H; Ar-H), 7.38–7.33 (m, 3H; Ar-H), 5.83 (s, 1H; PhCHOCO), 4.98–4.86 (m, 1H; CH₃CHOCO), 2.17 (s, 3H; CH₃CO), 1.81–1.37 (m, 8H; CH₂), 1.07 (d, ³J(H,H) = 6.0 Hz, 3H; CH₃), 0.97 ppm (t, ³J(H,H) = 7.5 Hz, 3H; CH₃); ¹⁹F NMR (282 MHz, CDCl₃): δ = -100.22 ppm; EI-MS: *m/z* (%): 177 (3); 149 (59); 135 (2); 118 (4); 107 (100); 43 (44); 28 (15); HRMS (ESI) [M+Na]⁺: *m/z* calcd for C₁₈H₂₄F₂O₄Na: 365.1540; found: 365.1547.

Compound (R)-3b': *R*_f = 0.90 (EtOAc/hexane 1:4); GC (isothermal, 140 °C; flow rate: 0.8 mL min⁻¹): *t*_R = 148 min; ¹H NMR (300 MHz, CDCl₃): δ = 7.47–7.43 (m, 2H; Ar-H), 7.36–7.31 (m, 3H; Ar-H), 5.83 (s, 1H; PhCHOCO), 4.85–4.77 (m, 1H; CHOCO), 2.15 (s, 3H; CH₃CO),

1.63–1.19 (m, 8H; CH₂), 0.87 (t, ³J(H,H)=7.2 Hz, 3H; CH₃), 0.78 ppm (t, ³J(H,H)=7.2 Hz, 3H; CH₃); ¹⁹F NMR (282 MHz, CDCl₃): δ = -101.58, -101.61 ppm; EI-MS: *m/z* (%): 177(3); 149 (59); 135 (2); 118 (4); 107 (100); 43 (44); 28 (15); HRMS (ESI) [M+Na]⁺: *m/z* calcd for C₁₈H₂₄F₂O₄Na: 365.1540; found: 365.1532.

Compound (S)-3b': *R*_f=0.90 (EtOAc/hexane 1:4); GC (isothermal, 140°C; flow rate: 0.8 mL min⁻¹): *t*_R=149 min; ¹H NMR (300 MHz, CDCl₃): δ = 7.47–7.43 (m, 2H; Ar-H), 7.36–7.31 (m, 3H; Ar-H), 5.81 (s, 1H; PhCHOCO), 4.85–4.77 (m, 1H; CHOCO), 2.15 (s, 3H; CH₃CO), 1.63–1.19 (m, 8H; CH₂), 0.95 (t, ³J(H,H)=7.2 Hz, 3H; CH₃), 0.57 ppm (t, ³J(H,H)=7.2 Hz, 3H; CH₃); ¹⁹F NMR (282 MHz, CDCl₃): δ = -101.58, -101.61 ppm; EI-MS: *m/z* (%): 177 (3); 149 (59); 135 (2); 118 (4); 107 (100); 43 (44); 28 (15); HRMS (ESI) [M+Na]⁺: *m/z* calcd for C₁₈H₂₄F₂O₄Na: 365.1540; found: 365.1532.

Compound (R)-4a': *R*_f=0.89 (EtOAc/hexane 1:4); GC (isothermal, 140°C; flow rate: 0.8 mL min⁻¹): *t*_R=174 min; ¹H NMR (300 MHz, CDCl₃): δ = 7.47–7.43 (m, 2H; Ar-H), 7.38–7.33 (m, 3H; Ar-H), 5.85 (s, 1H; PhCHOCO), 4.98–4.86 (m, 1H; CHOCO), 2.17 (s, 3H; CH₃CO), 1.78–1.28 (m, 8H; CH₂), 1.25 (d, ³J(H,H)=6.0 Hz, 3H; CH₃), 0.88 ppm (t, ³J(H,H)=6.0 Hz, 3H; CH₃); ¹⁹F NMR (282 MHz, CDCl₃): δ = -99.12, -99.17 ppm; EI-MS: *m/z* (%): 177 (3); 149 (59); 135 (2); 118 (4); 107 (100); 43 (44); 28 (15); HRMS (ESI) [M+Na]⁺: *m/z* calcd for C₁₈H₂₄F₂O₄Na: 365.1540; found: 365.1542.

Compound (S)-4a': *R*_f=0.89 (EtOAc/hexane 1:4); GC (isothermal, 140°C; flow rate: 0.8 mL min⁻¹): *t*_R=175 min; ¹H NMR (300 MHz, CDCl₃): δ = 7.47–7.43 (m, 2H; Ar-H), 7.38–7.33 (m, 3H; Ar-H), 5.82 (s, 1H; PhCHOCO), 4.98–4.86 (m, 1H; CHOCO), 2.17 (s, 3H; CH₃CO), 1.78–1.28 (m, 8H; CH₂), 1.09 (d, ³J(H,H)=6.0 Hz, 3H; CH₃), 0.93 ppm (t, ³J(H,H)=6.0 Hz, 3H; CH₃); ¹⁹F NMR (282 MHz, CDCl₃): δ = -99.12, -99.17 ppm; EI-MS: *m/z* (%): 177 (3); 149 (59); 135 (2); 118 (4); 107 (100); 43 (44); 28 (15); HRMS (ESI) [M+Na]⁺: *m/z* calcd for C₁₈H₂₄F₂O₄Na: 365.1540; found: 365.1542.

Compound (R)-5a': *R*_f=0.89 (EtOAc/hexane 1:4); GC (isothermal, 140°C; flow rate: 0.8 mL min⁻¹): *t*_R=255 min; ¹H NMR (300 MHz, CDCl₃): δ = 7.45–7.43 (m, 2H; Ar-H), 7.37–7.34 (m, 3H; Ar-H), 5.85 (s, 1H; PhCHOCO), 4.95–4.85 (m, 1H; CH₃CHOCO), 4.35 (dt, ²J(H,F)=4.8, ³J(H,H)=4.0 Hz, 2H; CH₂F), 2.17 (s, 3H; CH₃CO), 1.68–1.29 (m, 6H; CH₂), 1.22 (d, ³J(H,H)=4.0 Hz, 3H; CH₃), 1.22–1.11 ppm (m, 4H; CH₂); ¹⁹F NMR (282 MHz, CDCl₃): δ = -218.34 ppm; EI-MS: *m/z* (%): 177 (3); 149 (59); 135 (2); 118 (4); 107 (100); 43 (44); 28 (15); HRMS (ESI) [M+Na]⁺: *m/z* calcd for C₁₈H₂₅FO₄Na: 347.1635; found: 347.1637.

Compound (S)-5a': *R*_f=0.89 (EtOAc/hexane 1:4); GC (isothermal, 140°C; flow rate: 0.8 mL min⁻¹): *t*_R=258 min; ¹H NMR (300 MHz, CDCl₃): δ = 7.45–7.43 (m, 2H; Ar-H), 7.37–7.34 (m, 3H; Ar-H), 5.84 (s, 1H; PhCHOCO), 4.95–4.85 (m, 1H; CH₃CHOCO), 4.42 (dt, ²J(H,F)=4.8, ³J(H,H)=4.0 Hz, 2H; CH₂F), 2.17 (s, 3H; CH₃CO), 1.68–1.29 (m, 6H; CH₂), 1.22–1.11 (m, 2H; CH₂), 1.10 (d, ³J(H,H)=4.0 Hz, 3H; CH₃), 0.98–0.88 ppm (m, 2H; CH₂); ¹⁹F NMR (282 MHz, CDCl₃): δ = -218.34 ppm; EI-MS: *m/z* (%): 177(3); 149 (59); 135 (2); 118 (4); 107 (100); 43 (44); 28 (15); HRMS (ESI) [M+Na]⁺: *m/z* calcd for C₁₈H₂₅FO₄Na: 347.1635; found: 347.1637.

Determination of NADPH consumption rate:^[9b] Rate of NADPH consumption was determined by using a Beckman Coulter DU-800 UV/Vis spectrophotometer and a 1 cm path length cuvette. NADPH turnovers were carried out at 30°C in a reaction solution containing the purified enzyme (800 μL, 200 nm) in Tris-HCl buffer (100 mM, pH 8.2), bovine liver catalase (13 mg), and 4.0 mM substrate (added as a 400 mM stock solution in DMSO). P450 enzyme concentrations were determined by reduced CO difference spectra of the reduced heme by using an extinction coefficient of 91 mm⁻¹cm⁻¹ for the 450 minus 490 nm peak.^[9b,34] Assays were held for 1–2 min prior to NADPH addition at a final concentration of 320 μM, and the decrease in absorption at 340 nm was monitored. Rates were calculated based on the extinction coefficient of NADPH (6.22 mm⁻¹cm⁻¹). Background NADPH consumption rates were measured without substrates. All reactions were carried out in triplicate.

Determination of product throughputs or product formation rates:^[9b] NADPH (200 μL) to a final concentration of 320 μM was added to Tris-HCl buffer (100 mM, pH 8.2, 800 μL) containing purified protein (200 nm)

and 4.0 mM substrate in DMSO (1% v/v). After the enzymatic reaction proceeded for 1.0 min at 30°C (measurement of the initial oxidation rate), the reaction mixtures (1 mL) were quenched with CH₂Cl₂ (300 μL, with *p*-xylene as internal standard) and HCl (6.0 M, 100 μL) in a 2 mL microcentrifuge tube. The tube was vortexed and then centrifuged at 13000 rpm for 5.0 min. The organic layer was removed with a pipette and analyzed by GC to determine the product concentrations and throughput ratios. All reactions were carried out in triplicate.

Quantification of enzymatic alcoholic products was calibrated by the purified 2-alcohols **1–7a** or commercially available octan-2-ol (Sigma-Aldrich). The GC intensities of **1a–d**, **2a–c**, **3a**, and **3b** were determined by the calibration curve based on **1a**. Meanwhile, the GC intensities of **4a**, **5a–d**, **6a–c**, and **7a–d** were determined by the calibration curve based on **4a**, **5a**, **6a**, and **7a**, respectively. Aliquots of 2-octanol, **1a**, **4a**, **5a**, **6a**, and **7a** (0.03, 0.05, 0.10, 0.21, and 0.41 mg, respectively) were dissolved in CH₂Cl₂ (10 mL) containing xylene (0.43 mg). The corresponding GC intensity of standard alcohols was normalized by the intensity derived from xylene as the internal standard. The measured ratios of *I*_{alcohol} versus *I*_{xylene} then were fitted to a linear function of the weight of the alcohols that were added. The regressions for these linear plots from 0.01 to 0.50 mg were 0.997 to 0.999 and indicated that all the measurements within this range were valid.

Acknowledgements

This work was supported by Academia Sinica and grants from the National Science Council, R.O.C. (NSC 97-2113M-001-006-MY3 and 98-3114-E-006-014). We thank Dr. Mei-Chun Tseng for her assistance with ESI-MS.

- [1] L. O. Narhi, A. J. Fulco, *J. Biol. Chem.* **1987**, *262*, 6683–6690.
- [2] V. B. Urlacher, R. D. Schmid, *Methods Enzymol.* **2004**, *388*, 208–224.
- [3] S. N. Daff, S. K. Chapman, K. L. Turner, R. A. Holt, S. Govindaraj, T. L. Poulos, A. W. Munro, *Biochemistry* **1997**, *36*, 13816–13823.
- [4] R. Fasan, Y. T. Mehareenna, C. D. Snow, T. L. Poulos, F. H. Arnold, *J. Mol. Biol.* **2008**, *383*, 1069–1080.
- [5] V. B. Urlacher, R. D. Schmid, *Curr. Opin. Chem. Biol.* **2006**, *10*, 156–161.
- [6] a) M. W. Sawayama, M. M. Y. Chen, P. Kulanthaivel, M. S. Kuo, H. Hemmerle, F. H. Arnold, *Chem. Eur. J.* **2009**, *15*, 11723–11729; b) A. Rentmeister, F. H. Arnold, R. Fasan, *Nat. Chem. Biol.* **2008**, *5*, 26–28.
- [7] a) A. Cherkasov, M. Jonsson, *J. Chem. Inf. Comput. Sci.* **2000**, *40*, 1222–1226; b) S. Shaik, S. Cohen, Y. Wang, H. Chen, D. Kumar, W. Thiel, *Chem. Rev.* **2010**, *110*, 949–1017.
- [8] Q. S. Li, U. Schwaneberg, P. Fischer, R. D. Schmid, *Chem. Eur. J.* **2000**, *6*, 1531–1536.
- [9] a) M. W. Peters, P. Meinhold, A. Glieder, F. H. Arnold, *J. Am. Chem. Soc.* **2003**, *125*, 13442–13450; b) P. Meinhold, M. W. Peters, A. Hartwick, A. R. Hernandez, F. H. Arnold, *Adv. Synth. Catal.* **2006**, *348*, 763–772.
- [10] K. Y. Ng, L.-C. Tu, Y.-S. Wang, S. I. Chan, S. S.-F. Yu, *ChemBioChem* **2008**, *9*, 1116–1123.
- [11] a) H.-J. Böhm, D. Banner, S. Bendels, M. Kansy, B. Kuhn, K. Müller, U. Obst-Sander, M. Stahl, *ChemBioChem* **2004**, *5*, 637–643; b) K. Muller, C. Faeh, F. Diederich, *Science* **2007**, *317*, 1881–1886; c) S. Purser, P. R. Moore, S. Swallow, V. Gouverneur, *Chem. Soc. Rev.* **2008**, *37*, 320–330.
- [12] B. K. Park, N. R. Kitteringham, P. M. O'Neill, *Annu. Rev. Pharmacol. Toxicol.* **2001**, *41*, 443–470.
- [13] a) E. N. G. Marsh, *Chem. Biol.* **2000**, *7*, R153–R157; b) K. Ahn, D. S. Johnson, M. Mileni, D. Beidler, J. Z. Long, M. K. McKinney, E. Weerapana, N. Sadagopan, M. Liimatta, S. E. Smith, S. Lazerwith, C. Stiff, S. Kamtekar, K. Bhattacharya, Y. Zhang, S. Swaney, K. V.

- Becelaere, R. C. Stevens, B. F. Cravatt, *Chem. Biol.* **2009**, *16*, 411–420; c) R. Pongdee, H.-W. Liu, *Bioorg. Chem.* **2004**, *32*, 393–437; d) S. I. Chan, S. S.-F. Yu, *Acc. Chem. Res.* **2008**, *41*, 969–979.
- [14] a) R. P. Singh, J. M. Shreeve, *Synthesis* **2002**, 2561–2578; b) P. Kirsch, *Modern Fluoroorganic Chemistry-Synthesis Reactivity, Applications*, Wiley-VCH, Weinheim, **2004**.
- [15] W. H. Brown, T. Poon, *Introduction to Organic Chemistry*, 4th ed., Wiley, New York, **2010**.
- [16] K. S. Eble, J. H. Dawson, *J. Biol. Chem.* **1984**, *259*, 14389–14393.
- [17] Z.-Y. Long, Q.-Y. Chen, *Tetrahedron Lett.* **1998**, *39*, 8487–8490.
- [18] N. O. Brace, *J. Fluorine Chem.* **2001**, *108*, 147–175.
- [19] R. Cloux, E. Kováts, *Synthesis* **1992**, 409–412.
- [20] E. Weber, A. Seifert, M. Antonovici, C. Geinitz, J. Pleiss, V. B. Urlacher, *Chem. Commun.* **2011**, *47*, 944–946.
- [21] S. S.-F. Yu, L.-Y. Wu, K. H.-C. Chen, W.-I. Luo, D.-S. Huang, S. I. Chan, *J. Biol. Chem.* **2003**, *278*, 40658–40669.
- [22] D. Appel, S. Lutz-Wahl, P. Fischer, U. Schwaneberg, R. D. Schmid, *J. Biotechnol.* **2001**, *88*, 167–171.
- [23] D. C. Haines, D. R. Tomchick, M. Machius, J. A. Peterson, *Biochemistry* **2001**, *40*, 13456–13465.
- [24] G. Truan, M. R. Komandla, J. R. Falck, J. A. Peterson, *Arch. Biochem. Biophys.* **1999**, *366*, 192–198.
- [25] a) M. J. Cryle, J. J. De Voss, *Tetrahedron: Asymmetry* **2007**, *18*, 547–551; b) M. J. Cryle, N. J. Matovic, J. J. De Voss, *Tetrahedron Lett.* **2007**, *48*, 133–136.
- [26] H. Li, T. L. Poulos, *Nat. Struct. Mol. Biol.* **1997**, *4*, 140–146.
- [27] P. R. Ortiz de Montellano, *Chem. Rev.* **2010**, *110*, 932–948.
- [28] a) S. I. Chan, K. H.-C. Chen, S. S.-F. Yu, C.-L. Chen, S. S.-J. Kuo, *Biochemistry* **2004**, *43*, 4421–4430; b) S. J. Elliott, M. Zhu, L. Tso, H. H. T. Nguyen, J. H. K. Yip, S. I. Chan, *J. Am. Chem. Soc.* **1997**, *119*, 9949–9955.
- [29] T. C. Bruice, S. J. Benkovic, *Biochemistry* **2000**, *39*, 6267–6274.
- [30] G. B. Crull, J. W. Kennington, A. R. Garber, P. D. Ellis, J. H. Dawson, *J. Biol. Chem.* **1989**, *264*, 2649–2655.
- [31] Y. Nakagawa, K. Irie, R. C. Yanagite, H. Ohigashi, K. Tsuda, *J. Am. Chem. Soc.* **2005**, *127*, 5746–5747.
- [32] B. E. Smart, *J. Fluorine Chem.* **2001**, *109*, 3–11.
- [33] David R. Lide ed., *CRC Handbook of Chemistry and Physics*, 90th ed., CRC Press/Taylor and Francis, Boca Raton, **2010**.
- [34] a) S. C. Maurer, H. Schulze, R. D. Schmid, V. B. Urlacher, *Adv. Synth. Catal.* **2003**, *345*, 802–810; b) T. Omura, R. Sato, *J. Biol. Chem.* **1964**, *239*, 2379–2385.

Received: December 16, 2010

Published online: March 11, 2011